ISTANBUL TECHNICAL UNIVERSITY ★ GRADUATE SCHOOL

DEVELOPING A NOVEL ARTIFICIAL INTELLIGENCE BASED METHOD FOR DIAGNOSING CHRONIC OBSTRUCTIVE PULMONARY DISEASE

Ph.D. THESIS

İnanç MORAN

Department of Computer Engineering

Computer Engineering Programme

NOVEMBER 2023

ISTANBUL TECHNICAL UNIVERSITY ★ GRADUATE SCHOOL

DEVELOPING A NOVEL ARTIFICIAL INTELLIGENCE BASED METHOD FOR DIAGNOSING CHRONIC OBSTRUCTIVE PULMONARY DISEASE

Ph.D. THESIS

İnanç MORAN
(504072504)

Department of Computer Engineering

Computer Engineering Programme

Thesis Advisor: Prof.Dr. D.Turgay ALTILAR

NOVEMBER 2023

İSTANBUL TEKNİK ÜNİVERSİTESİ ★ LİSANSÜSTÜ EĞİTİM ENSTİTÜSÜ

KRONİK OBSTRÜKTİF AKCİĞER HASTALIĞI TEŞHİSİ İÇİN YAPAY ZEKA TABANLI YENİ BİR YÖNTEM GELİŞTİRİLMESİ

DOKTORA TEZİ

İnanç MORAN
(504072504)

İlgisayar Mühendisliği Anabilim Dalı

Bilgisayar Mühendisliği Programı

Tez Danışmanı: Prof.Dr. D.Turgay ALTILAR

KASIM 2023

İnanç MORAN, a Ph.D. student of ITU Graduate School student ID 504072504 successfully defended the thesis entitled "DEVELOPING A NOVEL ARTIFICIAL INTELLIGENCE BASED METHOD FOR DIAGNOSING CHRONIC OBSTRUCTIVE PULMONARY DISEASE", which he/she prepared after fulfilling the requirements specified in the associated legislations, before the jury whose signatures are below.

Thesis Advisor :	**Prof.Dr. D.Turgay ALTILAR** Istanbul Technical University	.....
Jury Members :	**Prof.Dr. Nafiz ARICA** Piri Reis University	.....
	Assoc.Prof.Dr. Yusuf YASLAN Istanbul Technical University	.....
	Prof.Dr. Mine Elif KARSLIGİL Yıldız Technical University	.....
	Prof.Dr. Mustafa Ersel KAMAŞAK Istanbul Technical University	.....

Date of Submission : **22 August 2023**
Date of Defense : **06 November 2023**

to my beloved wife Gamze and to my sons Doruk and Kerem,

FOREWORD

I'd like to thank the people below for supporting me with my PhD. I will always be grateful to them.

Prof.Dr. D.Turgay ALTILAR, my thesis advisor, I would like to express my sincere appreciation and gratitude for his exceptional personality, guidance, generosity, and support, all of which were essential to the development of this thesis. He has taught me many aspects of conducting research in the discipline of computer science. I owe him a huge debt of gratitude for teaching me how a CS research should be.

Prof.Dr. Nafiz ARICA, regarding this PhD, I would want to express my gratitude to him, a member of the thesis jury who provided me with helpful advice and ideas. In addition, I want to express my gratitude to him for the support, generosity, and direction he has provided.

Assoc.Prof.Dr. Yusuf YASLAN, I'd like to express my gratitude to him, a member of my thesis jury, for the guidance he's given me over the course of this PhD. Likewise, I appreciate his help and advice.

Additionally, I would like to extend my gratitude to the thesis defense jurors, Prof. Dr. Mine Elif KARSLIGİL and Prof. Dr. Mustafa Ersel KAMAŞAK, for their insightful evaluations, criticisms, and contributions that enhanced the quality of the thesis.

Lastly, I would like to thank my wife, my sons, my family and my friends for their support throughout my lengthy PhD program.

November 2023

İnanç MORAN
(Computer Engineer)

TABLE OF CONTENTS

ABBREVIATIONS

AI : Artificial Intelligence
ANN : Artificial Neural Network
AUC : Area Under the Curve
BP : Backpropagation
BAA : Broad Agency Announcement
CT : Computed Tomography
CNN : Convolutional Neural Network
COPD : Chronic Obstructive Pulmonary Disease
CWT : Continuous Wavelet Transform
DARPA : Defense Advanced Research Projects Agency
DL : Deep Learning
DNN : Deep Neural Network
ECG : Electrocardiogram
ELU : Exponential Linear Unit
FEV1 : Forced Expiratory Volume in 1 Second
FVC : Forced Vital Capacity
GAN : Generative Adversarial Networks
GOLD : Global Initiative for Chronic Obstructive Lung Disease
GPU : Graphical Processing Unit
kNN : K-Nearest Neighbor
LIME : Local Interpretable Model-Agnostic Explanations
ML : Machine Learning
mV : Millivolts
MRI : Magnetic Resonance Imaging
NN : Neural Network
ReLU : Rectified Linear Unit
RGB : Red-Green-Blue
SHAP : SHapley Additive exPlanations
ST : Stockwell Transform
STFT : Short-Time Fourier Transform
SVM : Support Vector Machine
TPU : Tensor Processing Unit
UWB : Ultra-Wideband
WT : Wavelet Transform
XAI : Explainable Artificial Intelligence

LIST OF TABLES

Page

LIST OF FIGURES

Page

DEVELOPING A NOVEL ARTIFICIAL INTELLIGENCE BASED METHOD FOR DIAGNOSING CHRONIC OBSTRUCTIVE PULMONARY DISEASE

SUMMARY

Today, research on machine learning and deep learning continues intensively due to their success in data classification and applications used in practice and their capacity to accurately reveal the information in the data. Since the beginning of the 21st century, especially deep learning, has produced very successful results by leaving traditional learning models behind and revolutionizing the latest technology. In this context, the detection of a fatal and global disease using deep learning has been researched in this thesis. The motivation of this research is to introduce the first research on automated Chronic Obstructive Pulmonary Disease (COPD) diagnosis using deep learning and the first annotated dataset in this field. The primary objective and contribution of this research is the development and design of an artificial intelligence system capable of diagnosing COPD utilizing only the heart signal (electrocardiogram, ECG) of the patient. In contrast to the traditional way of diagnosing COPD, which requires spirometer tests and a laborious workup in a hospital setting, the proposed system uses the classification capabilities of deep transfer learning and the patient's heart signal, which provides COPD signs in itself and can be received from any modern smart device. Since the disease progresses slowly and conceals itself until the final stage, hospital visits for diagnosis are uncommon. Hence, the medical goal of this research is to detect COPD using a simple heart signal before it becomes incurable. Deep transfer learning frameworks, which were previously trained on a general image data set, are transferred to carry out an automatic diagnosis of COPD by classifying patients' electrocardiogram signal equivalents, which are produced by signal-to-image transform techniques. Xception, VGG-19, InceptionResNetV2, DenseNet-121, and "trained-from-scratch" convolutional neural network architectures have been investigated for the detection of COPD, and it is demonstrated that they are able to obtain high performance rates in classifying nearly 33.000 instances using diverse training strategies. The highest classification rate was obtained by the Xception model at 99%. Although machine learning and deep learning generate accurate results, until a certain date, these techniques were subject to "black box" discourse. Recently, explainability has become a crucial issue in deep learning. Despite the exceptional performance of deep learning algorithms in various tasks, it is difficult to explain their inner workings and decision-making mechanisms in a way that is understandable. Explainable AI methods enable the accurate prediction of the outcomes of an AI model or the comprehension of the decision-making process. The LIME and SHAP methods, which are among the models that make it possible to interpret the results of deep learning and machine learning models, have been investigated for the purpose of interpreting the classifications made in the thesis. This research shows that the newly

introduced COPD detection approach is effective, easily applicable, and eliminates the burden of considerable effort in a hospital. It could also be put into practice and serve as a diagnostic aid for chest disease experts by providing a deeper and faster interpretation of ECG signals. Using the knowledge gained while identifying COPD from ECG signals may aid in the early diagnosis of future diseases for which little data is currently available.

KRONİK OBSTRÜKTİF AKCİĞER HASTALIĞI TEŞHİSİ İÇİN YAPAY ZEKA TABANLI YENİ BİR YÖNTEM GELİŞTİRİLMESİ

ÖZET

Günümüzde, veri sınıflandırmadaki ve pratikte kullanılan uygulamalardaki başarıları, verinin içindeki bilgileri doğru şekilde ortaya çıkarma kapasiteleriyle, makine öğrenmesi ve derin öğrenme üzerine araştırmalar yoğun şekilde devam etmektedir. 21. yüzyılın başından bu yana, özellikle derin öğrenme, geleneksel öğrenme modellerini geride bırakarak ve son teknolojide devrim yaratarak oldukça başarılı sonuçlar üretmektedir. Bu kapsamda, bu tezde, derin öğrenme kullanılarak ölümcül ve yaygın bir hastalığın tespit edilmesi üzerinde çalışılmıştır.

Bu doktora tezinin hedefi, etiketlenmiş kalp sinyali veri setini ve derin öğrenmeyi kullanarak Kronik Obstrüktif Akciğer Hastalığı (KOAH) teşhisini gerçekleştiren ilk yapay zeka araştırmasını ortaya koymaktır. Bu araştırmanın birincil katkısı, hastanın yalnızca kalp sinyalini (elektrokardiyogram, EKG) kullanarak KOAH'ı teşhis edebilen bir yapay zeka sisteminin geliştirilmesi ve tasarlanmasıdır. Hastane ortamında spirometre testleri ve zahmetli bir çalışma gerektiren geleneksel KOAH teşhisi yönteminin aksine önerilen sistem, derin transfer öğrenmenin sınıflandırma yeteneklerini ve KOAH belirtilerini kendi içinde sağlayan ve hastanın herhangi bir modern akıllı cihazdan alınabilen kalp sinyalini kullanmaktadır. Hastalık yavaş ilerlediği ve son aşamaya kadar kendini gizlediği için, hastaların tanı veya kontrol maksadıyla hastaneneye gitmeleri nadir görülmektedir.

Bu kapsamda, bu araştırmanın tıbbi amacı da, KOAH'ı tedavi edilemez hale gelmeden önce basit bir kalp sinyali kullanarak tespit etmektir. Daha önce genel bir görüntü veri seti üzerinde eğitilmiş olan derin transfer öğrenme yapıları, sinyalden görüntüye dönüştürme teknikleriyle üretilen hastaların elektrokardiyogram sinyal eşdeğer resimlerini sınıflandırarak KOAH'ın otomatik teşhisini gerçekleştirmek için kullanılmaktadır. KOAH tespiti için Xception, VGG-19, InceptionResNetV2, DenseNet-121 ve "sıfırdan eğitilmiş" konvolüsyonel sinir ağı mimarileri üzerinde çalışılmış ve 33.000'e yakın resim üzerinde farklı eğitim stratejileri kullanılarak yüksek sınıflandırma performansları elde edilebildiği gösterilmiştir. En yüksek sınıflandırma oranı 99%. ile Xception modeli tarafından elde edilmiştir. Bu araştırma, yeni tanıtılan KOAH tespit yaklaşımının etkili, kolay uygulanabilir olduğunu ve hastalığın teşhisi için bir hastanede yapılması gereken zahmetli tetkiklerin yükünü ortadan kaldırdığını göstermektedir.

Kronik Obstrüktif Akciğer Hastalığı (KOAH), tamamen geri döndürülemez bir hava akımı sınırlaması ile karakterize edilmiştir. Hem akciğerleri hem de kalbi önemli ölçüde etkilediği için, sanayileşmiş ve gelişmekte olan ülkelerde önde gelen hastalık ve ölüm nedenlerinden biridir. KOAH genellikle, sık ve uzun süreli sigara içiminden

kaynaklandığından, semptomlar genellikle hastalık ilerlediğinde ve kişi kötüleşerek hastaneye gittiğinde ortaya çıkar. Bu nedenle, erken KOAH tespiti klinik olarak önemlidir.

Tezin bir başka katkısı, geleneksel makine öğrenimi yöntemleri ve öznitelik çıkarma şemalarının aksine, alan bilgisi veya öznitelik seçme algoritması gerektirmeden zaman serisindeki kalp verilerini sınıflandırmasıdır. KOAH hastası ve sağlıklı deneklerin EKG zaman serisi sinyallerinden üretilen skalogramları kategorize etmek için önceden eğitilmiş olan derin ağların öğrenilmiş özelliklerini kullanan bir transfer öğrenme tekniği sunulmaktadır. Tezde, KOAH hastası ve sağlıklı bireylere ait EKG sinyalleri ile birlikte, Xception, VGG-19, InceptionResNetV2 ve DenseNet-121 gibi önceden eğitilmiş evrişimli sinir ağları kullanılarak KOAH'ın tespit edilmesine yönelik yöntemler üzerinde çalışılmaktadır.

Bu kapsamda, 12 bireyin 8'er saatlik EKG sinyali kayıtları alınmış, bu sinyaller 16 ve 32 saniyelik parçalara ayrılmış, sinyal dönüştürme yöntemlerini kullanarak resim formatına dönüştürülmüş ve ardından bu görüntüler derin konvolüsyonel ağlarda eğitim maksatlı kullanılmıştır. Xception, VGG-19 ve tarafımızca tasarlanan KOAH Dedektörü derin modellerinin EKG sinyallerinden KOAH tespitinde başarılı sonuçlar verdiği görülmüştür.

Makine öğrenimi ve derin öğrenme her ne kadar doğru sonuçlar üretse de, bu teknikler belli bir tarihe kadar "kara kutu" söylemine maruz kaldığı için, açıklanabilirlik son zamanlarda derin öğrenmede kritik bir konu haline gelmiştir. Çünkü, derin öğrenme algoritmalarının çeşitli görevlerde olağanüstü performans göstermesine rağmen, iç işleyişlerine ve karar verme mekanizmalarına ilişkin anlaşılır açıklamalar sağlamak zordur. Açıklanabilir yapay zeka yöntemleri, bir yapay zeka modelinin sonuçlarını güvenilir bir şekilde tahmin edebilme veya bir kararın arkasındaki nedenleri kavrayabilmeyi sağlamaktadır. Derin öğrenme ve makine öğrenmesi modellerinin ürettiği sonuçları yorumlamayı mümkün kılan bu modellerden LIME ve SHAP metodları, tez içeriğinde yapılan sınıflandırmaların açıklanması/yorumlanması kapsamında incelenmiş ve uygulanmıştır.

Tezde önerilen hastalık tespit yöntemi ileride pratik uygulamaya konulduğunda, EKG sinyallerinin daha detaylı ve hızlı yorumlanmasını sağlayarak göğüs hastalıkları uzmanlarının hastalığı teşhis edebilmesi için bir yardımcı araç işlevi de görebilecektir. EKG sinyallerinden KOAH'ı teşhis ederken elde edilen bilgi birikimi, hakkında çok az veri bulunan ve gelecekte ortaya çıkacak yeni hastalıkların da erken teşhisine yardımcı olabilecektir.

Son yıllarda, makine öğrenmesi ve derin öğrenme gibi teknolojiler, tıp alanındaki zorluklara yardımcı çözümler sunmada çok önemli bir rol oynamaktadır. Ayrıca, erken ve zamanında hastalık tespiti için tıbbi görüntülemenin öngörücü doğruluğunu da geliştirmektedirler. Tezin bir diğer motivasyonu, derin öğrenmeyi kullanarak KOAH hastalığı teşhisine yönelik ilk çalışmayı ortaya koyması ve aynı zamanda bu alandaki ilk etiketli veri setini kullanmasıdır.

Literatürde taranan önceki araştırmalara ilave olarak, tezde iki katkı sağlanmaktadır. Birincisi, derin transfer öğrenme kullanılarak elde edilen KOAH hastalığının düşük maliyetli, hızlı, güvenli ve otomatik tespitidir. KOAH'ın erken öngörülmesi hastalığın

ilerlemesini önlemede hayati önem taşıdığından, önerilen yöntem potansiyel hastalara erken bir aşamada hastalığı tespit etme ve tedavi olma fırsatı verecektir. İkinci katkı olarak, özellikle açıklanabilir yapay zeka ile elde edilen bulgular, gelecekte çıkarılacak olan özelliklerin potansiyel biyo-belirteç davranışlarının araştırılması gerektiğini göstermektedir.

Sonuç olarak, bu tez çalışması, araştırmaya konu olan bir dizi önemli alana ışık tutmuştur. Tezin başında belirtilen araştırma hedefleri detaylı olarak incelenmiştir. Önerilen yaklaşım derinlemesine değerlendirilmiş, ilgili literatür kapsamlı bir şekilde incelenerek dizayn edilen sistem ile başarılı sonuçlar elde edilmiştir. Bilgisayar mühendisliği ve biyomedikal alanlarında eş zamanlı ve önemli katkılarda bulunulduğu değerlendirilmektedir. Edinilen bulgular, ileride ayrıca yapılabilecek ilave araştırmalar için yeni yönler ortaya çıkarmış ve bu yönlerdeki potansiyel ilgi alanları vurgulanmıştır.

1. INTRODUCTION

Chronic Obstructive Pulmonary Disease (COPD) is defined by an irreversible restriction in airflow. It is one of the main causes of mortality and morbidity in both industrialized and developing nations because it affects both the lungs and the heart to a significant degree [1,2]. Since COPD is mostly caused by smoking cigarettes often and for a long time, symptoms usually show up when the disease has already gotten worse. Thus, early COPD detection is clinically important. The primary goal of this thesis is to diagnose COPD utilizing deep transfer learning methods and a simple heart signal in a practical and safe way, before the disease becomes incurable. Another contribution of this thesis is to classify time series heart data without requiring domain knowledge or a feature selection algorithm, as opposed to conventional machine learning methods and feature extraction schemes. A transfer learning technique is presented that employs the learned characteristics of pre-trained networks to categorize the scalograms produced from ECG time series signals of COPD and healthy subjects. Methods for automatic detection of COPD using ECG signals with a from-scratch model and pre-trained convolutional neural networks (CNNs) such as Xception, VGG-19, InceptionResNetV2, and DenseNet-121 are worked on.

The collected ECG signals of patients are converted from the time series domain to frequency-domain equivalent scalogram images using Wavelet and Stockwell transform. Afterward, to classify the scalograms, the power of pre-trained deep networks is utilized by transferring and fine-tuning. This is the first published research on COPD detection using ECG data utilizing deep transfer learning [3]. And this will also help the COPD diagnosis to be completed quickly since ECG signals are fairly simple to record in a typical healthcare facility or practically any household.

1.1 Purpose of the Thesis

In recent years, technologies such as machine learning and deep learning have played a crucial role in delivering assistive solutions to the challenges in the medical domain. Using these structures, the predictive accuracy for early and prompt disease detection is enhanced. As a result of the absence of qualified personnel, medical practitioners welcome such technological assistance, which enables them to treat more patients. In addition to critical health conditions such as cancer and diabetes, the social impact of respiratory diseases is gradually increasing and becoming life-threatening.

The motivation of this thesis is to introduce the first research on automated COPD diagnosis using deep learning and the first annotated dataset in this field. The primary objective and contribution of this thesis is the development and design of an artificial intelligence system capable of diagnosing COPD utilizing only the heart signal (electrocardiogram, ECG) of the patient.

1.2 Literature Review

This section introduces the applications of machine learning (ML) in COPD detection and examines the shortcomings and difficulties of current ML technology in light of the present state of research of ML technological advances commonly employed in the study of COPD.

When an individual is too sick to perform accurate pulmonary function tests, he or she must be evaluated based on his or her clinical features at the time. Peng et al. [4] gathered medical data and selected 28 variables, including vital signs, health history, multiple medical conditions, and various inflammatory signs. In addition, the effectiveness of the C5.0 model was assessed and found to be superior to that of the C4.5, regression and classification trees, and iterative dichotomous models. The study showed the C5.0 decision tree classifier did the best and allowed respiratory physicians to assess the severity of COPD in patients at the beginning more quickly using this classifier.

Chest computed tomography (CT) is an advanced imaging technique that is frequently used to detect abnormalities in lung texture and the status of COPD. However, chest

CT results provide a vast amount of image data from which pathophysiological abnormalities cannot be discerned. In recent years, supervised learning has been extensively developed and implemented in chest CT due to its ease of use, broad coverage, and high application performance. Support vector machines and logistic regression algorithms were used to assess the pulmonary ventilation function in COPD by analyzing chest CT images [5]. The validity of the assessment model (quadratic support vector machine) was evaluated in 27 COPD patients using 87 image features with an accuracy of 88% and an area under the curve (AUC) of 0.80. Similarly, Sun et al. developed lightly supervised deep learning models for the automated detection and staging of spirometry-defined COPD in the natural population using CT image data [6].

Another study [7] targeted to develop weakly supervised deep learning models that use computed tomography (CT) image data in order to automate the detection and staging of spirometry-defined COPD. The suggested chest method could automatically detect spirometry-defined COPD and classify patients using the GOLD scale. The attention-based model utilized for COPD detection yielded an AUC of 0.934 on the internal test set and 0.866 on the subset obtained from the National Lung Screening Trial. Using the GOLD scale, the multi-channel 3D residual network accurately classified 76.4% of COPD patients in the test set.

To detect COPD, another framework [8] was proposed that uses ultra-wideband (UWB) radar-based temporal and spectral characteristics of the patients to construct machine learning and deep learning models. A set of temporal and spectral characteristics are extracted from respiration data collected non-invasively from a distance of 1.5 meters using UWB radar. On the collected dataset, various machine learning and deep learning models were trained and evaluated. The outcomes were quite successful.

Using wearable devices, home air quality sensing devices, smartphone applications, and supervised prediction algorithms were able to make accurate predictions of future COPD events. A study was aimed to develop a prediction system based on lifestyle data, environmental factors, and patient symptoms for the early detection of COPD

within the next week [9]. Decision tree, random forest, k-nearest neighbor and deep neural network structures are used. Precision, sensitivity, specificity, and AUC were all greater than 0.90. Due to the limitations of air quality sensing devices, the scope of environmental collection is limited to the user's bedroom, implying that the predictive results are less accurate.

The lung sounds are physiological sound signals generated by the respiratory system of humans during exchange with the external environment, and they contain a wealth of physiological and pathological information. Using traditional stethoscopes, it is hard to record confident physiological sound signals, as well as the subjective experiences of physicians are capable of influencing the results of a diagnosis. Rapid advances in devices and artificial intelligence algorithms have made significant contributions to the analysis of breath sounds, aiding medical professionals in the diagnosis of respiratory illnesses and accurately determining the condition of patients with COPD. Altan et al. [10] proposed an approach that focused on lung sounds, and the research team examined 12 distinct lung sounds related to various levels of COPD degree of severity, evaluated the severity of COPD via multichannel pulmonary sounds, and utilized 3-D second-order distinction maps to identify abnormalities in lung sounds. Using cube and octet-based quantization techniques, the abnormal characteristics of chaotic maps were obtained. To predict the degree of severity of COPD, a classification was carried out employing a deep extreme learning machine classifier (Deep-ELM). The model's precision, sensitivity, and specificity were all greater than 0.90.

The aforementioned studies have some limitations: clinical tests performed on patients in different hospitals or by different doctors are not uniform, and there are differences in the number and significance of characteristics; depression, anxiety, and mobility are difficult to quantify. Each study model is only applicable to patients who meet specific criteria, and the models' generalizability is limited. Deep learning requires serious expenses for training and memory; an enormous quantity of data is needed to achieve solid model performance; as well as the "black box" characteristic of deep learning and machine learning may result in problematic outcomes [11].

Until very recently, most of the reported approaches in the literature for classifying the ECG signals solely relied on extracting hand-crafted features from the ECG [12]–[16]. This is performed by utilizing either traditional feature extraction algorithms or human expert knowledge. The extracted features are then fed either to generative or discriminative models to predict or classify the ECG signals. Support vector machines (SVMs) are widely utilized with hand-crafted features that have generated acceptable results among these approaches [17]. In this thesis, the extracted feature quality has the greatest influence on the reliability and performance of the classification approach.

Consequently, it is always sought to extract the disease's most representative, critical, dominant, and relevant characteristics. In addition, the ECG signal properties are subject-dependent, and the extraction of useful features often needs an in-depth understanding of the domain. Conventional feature extraction was regarded as an intrinsic component of ECG pattern classification. Recent research has demonstrated, however, that deep neural networks may do feature extraction straight from the data.

Other methods, including cosine transform, discrete Fourier transform, and wavelet transform, were additionally employed to derive characteristics from ECG signals both in the temporal and the frequency domains [18]. Classification of time series data is one of the most recent uses of deep neural networks. In a variety of applications involving health care systems, bioinformatics, recognition of activities, etc., time series classification problems involving voluminous amounts of data are used. Diverse techniques, such as deep belief networks, recurrent neural networks, conditional and gated restricted Boltzmann machines, autoencoders, hidden Markov models (HMMs), and convolutional neural networks (CNNs), have all been employed and developed in the scientific literature to tackle identical time series data classification problems to the ECG classification [19,20].

The framework for deep learning enables the network to discover the optimal characteristics for a specific task. There have been several documented applications of deep transfer learning in health informatics [21]–[30]. Specifically, deep learning experiments with ECG signals include the diagnosis of arrhythmia [31,32], congestive heart failure [33], atrial fibrillation [34] and other cardiac disorders. In

these investigations, deep learning outperformed conventional methods and offered additional benefits, including the elimination of the necessity for feature extraction, feature selection, and de-noising.

Not much research has been conducted on the use of ECG for COPD detection. Thus, we conducted a research to demonstrate the usefulness of heart signal data in COPD diagnosis [35]. After gathering ECG signal data from the individuals with and without COPD, twenty four distinct ECG characteristics were derived in the time domain. Since the ECG is a biological signal and does not have a normal distribution, the Mann-Whitney U test was employed to examine whether the ECG characteristics of the patient and control groups were substantially different. If the value received from the test result is not statistically significant, the result is considered significant, indicating that there is a difference between the groups. The research concluded that the ECG signal can be used as a discriminator for COPD disease. Consequently, we presented a new COPD diagnostic approach employing a rule-based machine learning method utilizing an ECG signal [36]. According to the classification results of the decision tree method, the disease condition may be diagnosed with 93.89 percent accuracy. At the beginning of this thesis, after getting the images that were transformed (the transformation method will be explained in Chapter 4) from the ECG signals, we also tried to utilize the kNN algorithm to classify the COPD from these images. As another machine learning method, we utilized the kNN algorithm which gave succesful results, with 93.00 percent accuracy. Following these results, we aimed to improve the classification result using deep learning rather than traditional machine learning techniques, and we began investigate to diagnose the disease in question using deep learning.

1.3 Organization of the Thesis

Beyond the introduction, there are five more chapters in this dissertation. In order to familiarize the reader with COPD, the nature of the ECG signal, and its relationship with COPD, some beginner level background information is presented in Chapter 2.

In Chapter 3, the fundamentals of deep transfer learning are presented. This chapter is intended for non-experts and can be bypassed if the reader is already familiar with deep learning's basic concepts and techniques.

Following, in Chapter 4, giving insight on the proposed architecture design, data collection, data production, wavelet and Stockwell transform methods and deep transfer learning strategies used in the thesis.

Chapter 5 presents the obtained results and the analysis. Limitations and experimental setup utilized in this thesis are given. Comparative findings from the various experimental configurations and the explainable artificial intelligence projections are reported in this chapter.

Finally, a review of the study, conclusions and some additional insight towards future studies are provided in Chapter 6. The chapter describes the best performing models and how the knowledge and experience obtained in this work may be applied to other illness detection or classification problems besides COPD.

2. BACKGROUND

In this chapter, background concepts essential to comprehending this dissertation are explained. Following the introduction of COPD, the nature of the ECG signal and the correlation between COPD and the ECG signal will be addressed.

2.1 Chronic Obstructive Pulmonary Disease

According to the World Health Organization, chronic obstructive pulmonary disease (COPD) will be the third-leading cause of death and the seventh-leading cause of morbidity worldwide by 2030 [37]. Acute flare-ups of chronic obstructive pulmonary disease are associated with a faster decline in lung function, a lower quality of life, and an increased mortality risk. In the entire world, COPD is underdiagnosed. COPD can be better managed and death rates can be lowered if it is found early and correctly. In recent years, there has been a lot of progress in the development and use of machine learning (ML), which is an important part of predictive analytics that uses predictive models that get better as the number of cases increases, to find better ways to deal with COPD.

According to the Global Initiative for Chronic Obstructive Lung Disease (GOLD) criteria, COPD is defined as; forced expiratory volume in 1 second (FEV1) divided by forced vital capacity (FVC) being smaller than 0.70 [1]. Today, a classical COPD diagnosis is made by using some clinical applications like spirometer tests, static lung volumes, exercise testing, ECG, echocardiography, magnetic resonance imaging (MRI) and computed tomography (CT). The majority of these procedures can be performed with considerable effort in a hospital or well-equipped medical facility. To effectively interpret the spirometer, CT, and MRI, well-trained experts with the necessary skills and expertise are required. This time-consuming and effort expensive condition may discourage future COPD patients from seeking hospital care while the disease is progressing. As a result, it is clear that early, practical, and safe diagnosis of

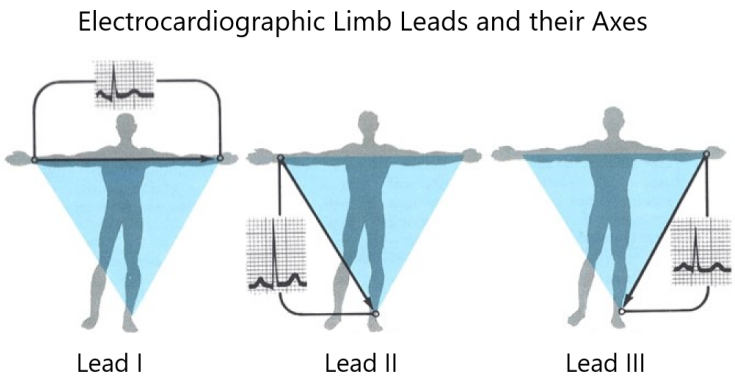

Figure 2.1 : Placement of the ECG electrodes in Lead I-II-III.

COPD disease is extremely beneficial to human health. This goal serves as the impetus for this thesis.

2.2 Nature of the ECG Signal

To begin at the beginning, an electrocardiogram is a visual representation of the electric waves generated by the heart during cardiac action. It provides information on the pace, rhythm, and shape of the heart. Using electrodes placed on the skin, an ECG graphs the electrical activity of the heart as a function of time. Fig. 2.1 depicts the placement of the electrodes in Lead I-II-III on a patient's body. These electrodes detect the tiny electrical changes caused by depolarization and repolarization of cardiac muscle throughout each cardiac cycle (heartbeat).

Fig. 2.2 illustrates the three principal components of an ECG. P wave reflects atria depolarization, QRS complex reflects ventricle depolarization, and T wave reflects ventricle repolarization. All of the waves and intervals in an ECG signal have a predictable time length, a range of acceptable amplitudes (voltages), and a standard morphology. Any deviance from the normal track has the potential to be unhealthy and, consequently, has clinical significance. ECG analysis offers a variety of beneficial uses, including activity recognition, biometric identification, patient screening, and diagnosis. Due to its non-invasive nature and low cost, the ECG is the most popular and essential diagnostic tool for the assessment of almost all diseases in clinical routine.

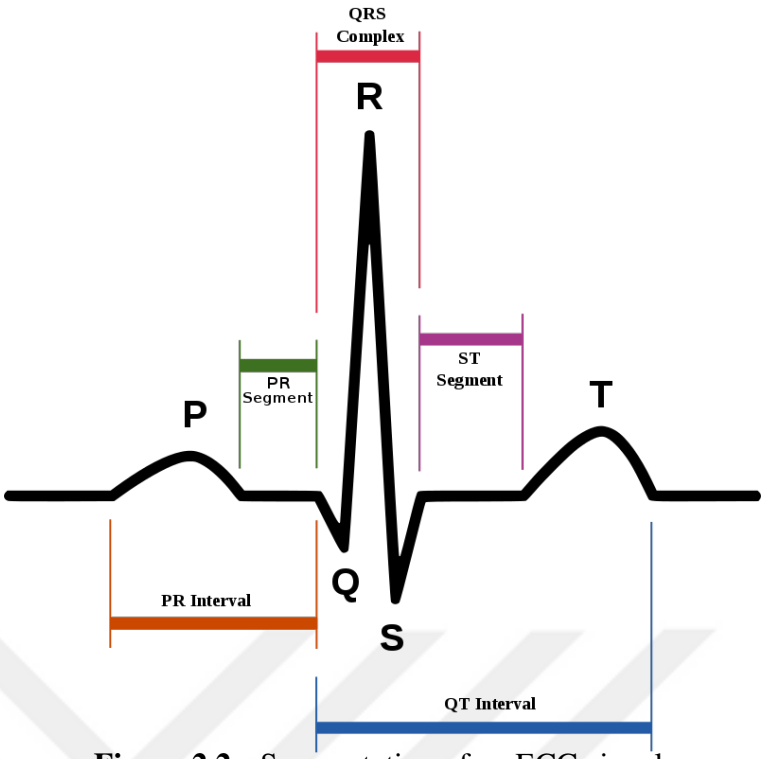

Figure 2.2 : Segmentation of an ECG signal.

2.3 Correlation Between COPD and the ECG Signal

There are a number of studies whose goals are to examine the connection and association between respiratory function and ECG characteristics among individuals with COPD and find out the results of the ECG that can indicate the presence of COPD [13,14,38]. The major findings of these studies are:

• QRS amplitude in Lead-I was significantly correlated with airflow limitation determined by FEV1/FVC.

• The multivariate analysis identified the QRS amplitude in Lead-I as an independent variable associated with COPD

• When suspecting COPD-related ECG changes, observe a moderate rise in the heart rate, a vertical P-axis, a small P-wave in v1, tiny QRS amplitudes, a QRS-axis that is vertical or slightly deviated (typically to the left), and a clockwise rotation of the precordial (horizontal) QRS transition region

COPD disease indirectly affects the heart conditions, and corresponding heart abnormalities can be detected by trained physicians. Some of these heart abnormalities include:

• Reduced lung conductivity as a result of hyperinflation

• Increase of anteroposterior chest diameter (increase of distance between heart and chest electrodes)

• Replacement of diaphragm downwards

• Chest electrodes' staying above because of replaced diaphragm

• Hypertrophy and dilation of the right ventricles dependent on pulmonary hypertension

• Vertical heart as a result of diaphragm and heart replacement downwards.

It is plausible to assume that each of these pathophysiological mechanisms could affect the heart and the electrical conduction of the thorax. Consequently, physical anomalies influence the nature of the ECG signal as follows:

• P wave verticalization's growing beyond +60°

• At the point where the P wave axis hits 90 degrees, a straight P wave develops in the Lead-I sign

• Verticalization of the P wave is correlated with obstructive lung function. Near the inferior vena cava, a pericardial ligament links the right atrium to the diaphragm. While the diaphragm descends and gradually flattens, the right atrium descends and the P wave transforms vertically. The verticalization of the P wave on the electrocardiogram is one of the most significant indications observed during COPD surveillance.

• Low peak-to-peak amplitude. The decrease in conductivity of the lungs as a result of hyperinflation and the increased distance between the chest electrodes and the heart causes this situation.

• As a result of the replacement of the diaphragm downwards and thus the verticalization of the heart, the QRS axe's verticalization and shifting to the right.

• Stenosis of QRS complex, due to left ventricular non-usage atrophy and low voltage

• Loss of R progression in the anterior

• Heart verticalization due to the diaphragm being replaced downwards

• The chest electrodes' staying relatively above because of the diaphragm being

replaced downwards

• Atrial arrhythmias (seen especially in the decompensation period of COPD)

• QS wave (between V1-V3) at right precordials

• T wave's becoming more evident, especially if P wave is high.

Several investigations involving COPD patients have revealed characteristic alterations in their ECG signals. Studies have revealed that the P axis is useful for detecting COPD, and the verticalization of the P wave has been proven to correlate with COPD. In addition, a larger P wave in Lead-III than in Lead-I has been reported as a screening marker for emphysema [39]. Recent reports [40]–[43] indicate that a vertical P axis greater than 60 is a helpful marker for COPD. Lead-I frequently displays a low QRS voltage in COPD patients [41]. "Lead-I sign" refers to a Lead-I QRS amplitude smaller than 0.15mV [44,45]. The nearly perpendicular frontal plane of the QRS axis in Lead-I of COPD patients leads to a low QRS amplitude in Lead-I. The low QRS voltage in Lead I is a result of the isolating effect of hyperinflated lungs as well as the heart's lower position relative to the electrode placement. These investigations suggest that the anomalies described in the ECG signal of a COPD patient are useful diagnostic criteria for COPD.

3. DEEP TRANSFER LEARNING

In this chapter, important background concepts for the understanding of deep transfer learning will be explained. Firstly, general machine learning topics are given. Afterwards, deep learning concept will be given consequently.

3.1 Machine Learning

Fundamentally, machine learning is a subfield of artificial intelligence (AI) in which a prediction algorithm is constructed [46]. The difference between traditional AI and machine learning is that machine learning algorithms are trained solely on data, as opposed to human instructions, so that they appear to learn autonomously. Arthur Lee Samuel [47] created the term Machine Learning in 1959. Training is the process of adjusting a model to fit a particular problem. In machine learning, the typical goal is to find a mapping from input patterns to an output value [48].

This mapping between the values of the input and output is typically an extremely intricate and nonlinear function which cannot be discovered by machine learning algorithms that can only discover linear mappings. In order for the algorithm to find an easier mapping between these features and the output value, researchers model data employing hand-optimized features. However, this strategy requires the generation of new hand-optimized features for every new task, and the creation of these features is a complex and challenging process.

Typically, the so-called training set is used for setting the machine learning model's parameters [48]. This training set includes n input vectors and, if desired, n target vectors (one for each sample). During the training phase, also referred to as the learning phase, the model's parameters that determine the mapping between the input vector and output value are adjusted. Following the training phase, the test set is utilized to determine the model's quality. Generalization is a model's ability to foresee the target value of new (unknown) samples with precision. Generalisation is the

method of generating an output from an unknown set of inputs using the data a model has been trained with, as the model generalises the patterns of the data it has learned to new data. If the output is a label for the input, then the model is solving a classification problem; if it is a value for the input, then it is solving a regression problem. In theory, classification is a kind of regression in which the model produces an integer value, but the two are typically distinguished. In both cases, the goal of the model is to approximate as accurately as possible the actual value of each input. This is known as the ground truth. When the ground truth is known, the learning process is said to be supervised [46]. This additional data enables the model's performance to be calculated using a metric that compares the discrepancy between the ground truth and the model's prediction. This is the model's error function. Learning is considered unsupervised when the ground truth is unknown. This is frequently the case when acquiring labelled data is prohibitively expensive. One of the applications of machine learning models for these problems is data clustering. That is, to determine a decision boundary between data points so that highly related data points are grouped together. They are also used to reduce the dimensionality of complex problems.

3.1.1 Machine learning algorithm types

To give a general aspect of machine learning, various settings of ML are presented in Fig. 3.1 and described in more detail below. The following describes how the algorithm type is determined by the features of the data collection and the particular task.

Supervised learning: The problem of supervised learning is a classic scenario for machine learning [48]. The training data consists of tuples $(x_i;y_i)$, where x_i is the input vector and y_i is the target vector. Classification problem refers to the situation in which the objective value is discrete, such as in the digit recognition problem, and the images are mapped to a finite number of discrete categories. The task is referred to as a regression problem if the objective value is continuous. The prediction of the price of a house (continuous output value) based on the number of rooms and the living area would be an example of a regression problem.

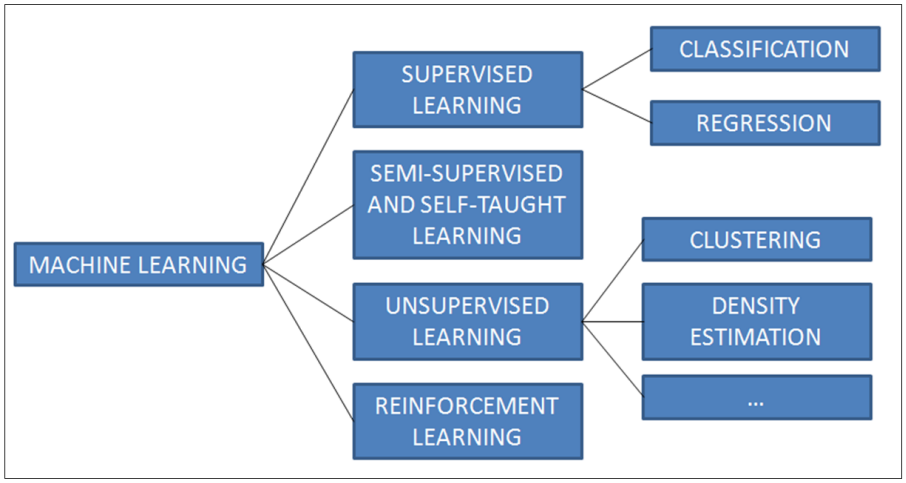

Figure 3.1 : Overview of machine learning settings.

Unsupervised learning: In unsupervised learning problems, instances of input vectors without target values are used as training data [48]. The objectives of unsupervised learning problems include clustering, density estimation, and visualization. Clustering's purpose is to locate groups of similar instances depending on their calculated or assumed similarities. The primary goal of density estimation is to figure out the data distribution inside the input space. For visualization, the data is projected from a high-dimensional space to either two or three dimensions.

Semi-supervised and self-taught learning: Two approaches are a compromise between supervised and unsupervised learning because they use unlabeled data in supervised learning tasks. The ability of methods to learn from unlabeled data and the difficulty of acquiring labeled data for supervised learning tasks serve as driving factors for these approaches. The primary objective is to provide the algorithm with a large amount of unlabeled data to learn a good feature representation of the input, followed by labeled data to carry out the supervised task using the learned feature representation [49]. In semi-supervised learning, the training data set can be split into two parts: the data samples $X_l = \{x_1,....x_l\}$ with corresponding labels $Y_l = \{y_1,....y_l\}$, and the data samples $X_u = \{x_{l+1},....x_{l+u}\}$ for which the labels are not known. Self-taught learning is more successful than semi-supervised learning because, unlike semi-supervised learning, it does not assume that the unlabeled data follow the same distribution (or class labels) as the labeled data X_u. As an illustration of the difference between the two approaches stated, we can consider a scenario in which the objective

is to distinguish between photos of cats and images of dogs. Both techniques employ labeled images, each of which depicts either a dog or a cat. This kind of setup is referred to as semi-supervised if the unlabeled data examples include all images of either a cat or a dog, but are unlabeled. In contrast, the unlabeled data set in self-taught learning consists of random images (obtained from the Internet) and thus comes from a different distribution than the labeled data set.

Reinforcement learning: Reinforcement learning deals with the question of how to interact with the environment and choose appropriate behaviors in a given situation so as to maximize the reward [48]. In unsupervised learning, unlike supervised learning, there are no scenarios of the optimal output; rather, the algorithm ought to discover which actions to take in a given scenario by interacting with its environment.

3.1.2 Hyperparameters

According to Bengio [50], the hyperparameter issue is as follows:

"We define a hyperparameter for a learning algorithm 'A' as a value to be selected prior to the actual application of 'A' to the data, a value that is not directly selected by the learning algorithm itself."

So, selecting hyperparameters is formally almost equal to selecting a model, i.e. selecting the best value or algorithm from a set of available options. Hyperparameters can be thought of as an external control button and can be continuous (learning rate) or discrete (the amount of neurons in one layer). In some cases, the number of hyperparameters can be relatively high (ten or more), which complicates the matter [50]. For all the learning algorithms examined in this work, hyperparameters had to be adjusted. The hyperparameters used in the experiments of this thesis will be explained in chapter 5.2 in detail.

3.1.3 Data utilization methods

Due to the issue of overfitting, the training set is not a reliable indicator to assess the predictive performance of various values for the parameters. Instead, the dataset can be split into three parts if there is enough data. The initial portion of the data, referred to as the training set [48], is used to train the model with various hyperparameter settings. The validation set is a collection of independent data. Since this second portion of the data is not used for training, it may be used to compare the several hyperparameter settings and choose the one that has the greatest score for predictive performance. A third portion of the data, referred to as the test set, is required to finally assess the selected model in terms of generalization. This is because the final model was chosen using the validation set, which means that the validation set is no longer completely independent from the model and overfitting to the validation data can happen.

Cross-validation is another approach that splits the dataset into two parts: the training set and the test set. This method is particularly useful when the amount of data is constrained and training should make use of as much of the available data as possible . Cross-validation comes in a variety of forms, but they all have the same fundamental concept. K-fold cross-validation, which randomly divides the training set into k groups, is a popular type [48]. A set of models are trained on k-1 groups and then evaluated on the remaining group. Each group goes through this procedure once more, resulting in a final evaluation of every group. The model is chosen based on the aggregate performance scores obtained from all runs. The performance of the chosen model is then assessed using the test set. In addition to the k-fold cross-validation method, another particular form is the leave-one-out method, where k is set to be the same as the number of samples. Cross-validation has the disadvantage of increasing the number of training runs (for a single setup) by the factor of k.

3.2 Deep Learning

This section provides a general introduction to deep learning. After giving the issues about its emergence and development, it is described why deep learning approaches

can be advantageous, as well as the central concepts of deep architectures and the motivations for employing them. In addition to focusing on this general part, this chapter describes the deep transfer learning method, which is evaluated in this thesis and given the implementation details in the next chapter.

The major advance that followed the launch of AlexNet [51] regarding the selection of a framework for image classification developed the Convolutional Neural Network (CNN) model as the most successful base model in the field to date. By substantially surpassing every other previous version at the time of its introduction in 2012, with a top-five error percentage of 17%, it quickly acquired popularity and paved the way for the image detection research challenge, as the next best opponent model could only achieve 26.8%. Yann Lecun first proposed the concept in his 1998 paper [52]. Lecun however used the concept to the categorization of documents and not images. Furthermore, the technology available at the time was not sufficient to train a model as large as a CNN, so the idea was abandoned up until AlexNet was born. Fig. 3.5 illustrates the architecture presented in [51]. After AlexNet in 2012, the industry experienced an expansion boom with major enhancements each year based on the CNN model. Presented in 2014 [53], given a more intuitive and complete explanation of the CNN structure.

The year that followed, in 2014, VGGNet [54] achieves an error rate of just 7.2%.This represents an important advance over the competition's state of the art. This article shows how increasing network depth can circumvent the optimization of hyperparameters which influence the network's architecture, such as kernel and padding size, the amount of convolutional layers per pooling layer, and others. It emphasizes the significance of depth in capturing hierarchical characteristics. In the period that followed, both Microsoft and Google entered the competition with Resnet and GoogLeNet, respectively. GoogLeNet [55] also entered the competition in 2014, with an error rate of 6.7%, simply pushing out VGG.

Google reduced the error rate to 3.08 percent in 2016. This network, unlike VGG, comprised 22 convolutional layers, some of which functioned in parallel. Due to the extreme complexity of the model, it was difficult for researchers without the resources

of an enterprise like Google. GoogLeNet utilized the Network In Network [56] approach, which employed 1x1 convolutions as a form of reduction in dimensionality whereas preserving the complex maps of features extracted by the convolutional layers. The result is that the model incredibly compact and efficient. GoogleNet's parallelism was significant because of its usefulness for distributed computing. By showing that non-sequential layer stacking surpasses stacked structures, dependability on distributed computing is established.

In the year 2015, Microsoft's ResNet [57] went into the contest and won with a score of 3.6%, reducing by half the previous record as well as surpassing human error for the first time. This system, which also got the record for the number of layers with 152, carried on the legacy of the VGG by proving that computing power could solve almost any issue. To reach the performance showed at the contest, training the neural network on a computer with eight GPUs continued to take more than two weeks. Nonetheless, this network was important for the state of the art because it introduced a new system for avoiding overfitting, which was obviously necessary for architectures of this depth. This design added the outcomes of the pooling and convolutional layers to the input. This led to the formation of a residual block, an innovative structure that allowed information to be passed across the layers without being entirely transformed at every layer.

Regional-CNN [58], also referred to as R-CNN, was an important advancement to the field as it combined methods for segmenting images with CNNs to significantly enhance computer vision object detection. R-CNN, the progenitor of multiple models that enhanced its computational efficiency (Faster R-CNN in citeGirshick2 and even Faster R-CNN in citeRen2017), established the learning skills of CNNs in object detection by first employing methods for image segmentation such as Selective Search, which divided the image into regions of interest, then integrating a CNN on those regions to determine the existence of the object. The study published in 2017 by the Facebook research team [59] introduced an approach to predict a pixel-level mask for detecting objects in a picture in parallel with the bounding-box method of Faster R-CNN before feeding it to a CNN. This method outperformed each additional

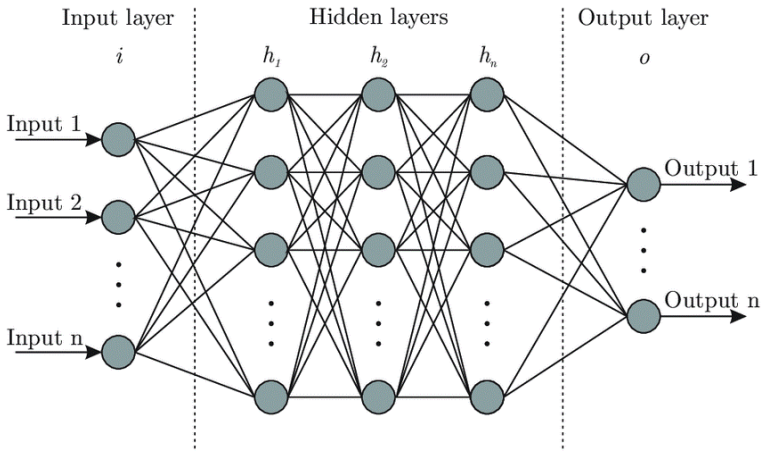

Figure 3.2 : Traditional artificial neural network structure.

single-model entry in the COCO challenge suite, the benchmarking test suite for object detection.

3.2.1 What is "deep" ?

Deep learning belongs to the class of machine learning methods. It is a specialized form of representation-based learning in which a network learns and constructs intrinsic features from each successive hidden layer of neurons. In contrast to shallow learning, in which both input and output are typically closely linked, deep learning defines the connection among input and output by processing the input through several intermediate processing layers [60]. Deep learning emphasizes the use of deep neural networks, which are neural networks with multiple hidden layers between the input and output layers. These deep architectures enable the networks to learn complex patterns and representations.

Deep model learns the features of the input set iteratively, resulting in automated feature extraction and selection. The term “deep” is derived from the numerous hidden layers in the Artificial Neural Network (ANN) structure. The structure of the neural network is depicted in Fig. 3.2.

Deep learning techniques have gained popularity due to their ability to model complex problems where hand-crafted features have proven to be overly simplistic [51]. The intermediate layers that separate the input layer and the output layer in deep learning are referred to as hidden layers. Every neuron or node (nerve cell) is connected to each

neuron in the next layer through a connection link. A nerve cell is made up of axon (output), dendrites (input), a node (soma), nucleus (activation function), and synapses (weights). The greater the number and size of a network's hidden layers, the more complicated the model and the more complicated the features it can capture. This necessitates additional data and computing power for their learning. This trade-off is another explanation why these models have only recently gained popularity, as the number of available datasets has multiplicatively increased due to the development of fields like Big Data.

3.2.2 Deep architectures

Deep architectures include abstraction and representation levels that enable the modeling of high-dimensional, nonlinear data such as images, audio, and text. Here, abstractions can be understood as categories or as discrete or continuous features [61]. Deep learning is primarily concerned with discovering automatically abstractions from low-level features to high-level representations. This learning procedure should be carried out with minimal human intervention and without hand-engineering of features. There are numerous advantages and motivations for implementing deep architectures. Due to their exceptional capabilities, deep learning architectures have grown in popularity and been beneficial in many fields. The following are some benefits and reasons to use deep learning architectures:

Ability to learn from large amounts of data: Deep learning models are exceptionally good at digesting massive volumes of data and identifying insightful patterns. They have the ability to autonomously learn complex representations and features from unstructured data, which is very useful in fields with big datasets, such speech recognition, natural language processing, and image recognition.

Feature extraction and representation learning: Deep learning architectures can automatically learn hierarchical data representations using feature extraction and representation learning. A deep neural network can recognize complicated patterns and correlations in the data because each layer learns to extract increasingly complex information. By doing away with manual feature engineering, time and effort are saved.

Better performance on complex tasks: Deep learning models have surpassed traditional machine learning methods in a number of complex tasks, achieving state-of-the-art performance. Deep learning architectures have substantially aided tasks like sentiment analysis, image and speech recognition, natural language understanding, machine translation, and sentiment analysis.

End-to-end learning: Deep learning makes it possible for a model to learn to carry out a task from the initial input to the final output. As a result, manual preprocessing and intermediary steps are not required, simplifying and improving the pipeline as a whole.

Generalization skills: Deep learning models have displayed amazing generalization skills, which means they can successfully process data that has not yet been seen or that comes from a different distribution than the training set. This makes it possible for the models to effectively generalize to and adapt to real-world events.

Flexibility and adaptability: Deep learning systems can handle a variety of data formats, including images, text, audio, and video, and are very flexible. By changing the design or training procedure, they may be tailored to different problem domains, making them adaptable for a variety of applications.

Continuous learning and transfer learning: Continuous learning and transfer learning: Deep learning models can be trained gradually and updated with fresh data, enabling them to adjust to shifting surroundings and draw knowledge from growing datasets. Transfer learning methods also eliminate the requirement for extensive training on sparse data by allowing the reuse of previously taught models on similar tasks.

Deep learning architectures have been widely used in a variety of sectors, transforming industries including computer vision, natural language processing, autonomous systems, healthcare, finance, and many others because to these benefits and drivers.

3.2.3 Deep neural networks

The neural network of the human brain, namely, is the source of inspiration for artificial neural networks [62]. In this subsection, general principles of neural networks, such

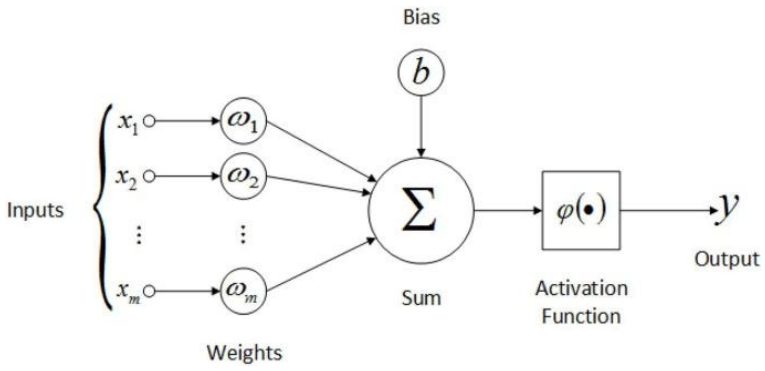

Figure 3.3 : Artificial neuron structure.

as neurons, weights, and activation functions, are explained in order to first be able to model non-linear data.

Neural networks are composed of individual neurons that are interconnected and, as a result, form the neural network [63]. A neuron is the fundamental component of a neural network and can be viewed as a simple model. The fundamental structure of a neuron is depicted in Fig. 3.3. Figure Fig. 3.3 depicts a neuron that receives multiple inputs X_i and computes the output as follows:

$$output = f(\sum_{i=1}^{m} w_i x_i + b) \tag{3.1}$$

where the parameters w_i are defined as weights, the parameter b as bias and f(.) is a nonlinear activation function [48]. The output of a neuron is also called activation. The activation function in the artificial neuron acts as the nucleus in a biological neuron whereas the input signals and its respective weights model the dendrites and synapses, respectively.

Every input value x_i in this computation is weighted, and as a result, multiplied by a unique weight w_i. The bias parameter allows for the addition of an offset to the data, and the weighted input values and bias b are added together. The final output of the neuron is obtained by transforming the outcome of this linear combination using the nonlinear activation function [63]. This introduction of nonlinearity is required [61] in order to locate nonlinear mappings. Common choices in machine learning for the nonlinear activation function are the logistic sigmoid function:

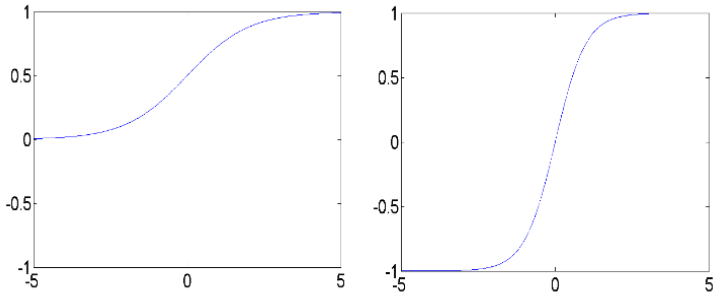

Figure 3.4 : Nonlinear activation functions.

$$f(x) = \frac{1}{1+e^{-x}} \tag{3.2}$$

and the hyperbolic tangent function:

$$f(x) = tanh(x) = \frac{e^{x} - e^{-x}}{e^{x} + e^{-x}} \tag{3.3}$$

which are depicted in Fig. 3.4.

An activation function in the context of deep learning is a function which employs a transformation to the output of a neural network layer. The objective of an activation function is to map the output, that may have any value between negative and positive infinity, to a more practical value. This function is employed to introduce non-linearity in the hidden layers via ReLU and ELU activations. In classification problems, the output layer usually gets activated by functions like Softmax, which restrict the output between 0 and 1 to convey the probability distribution between classes.

3.2.4 Convolutional neural networks

A problem with data that is high-dimensional, like images, is that the memory and processing needs of a great number of models become too high. In a neural network, the number of connections among neurons increases exponentially, causing problems with memory and computing. CNNs are a kind of neural networks which have been developed for processing image data and have additionally been used for speech and text recognition. The input layers are processed through convolution layers which

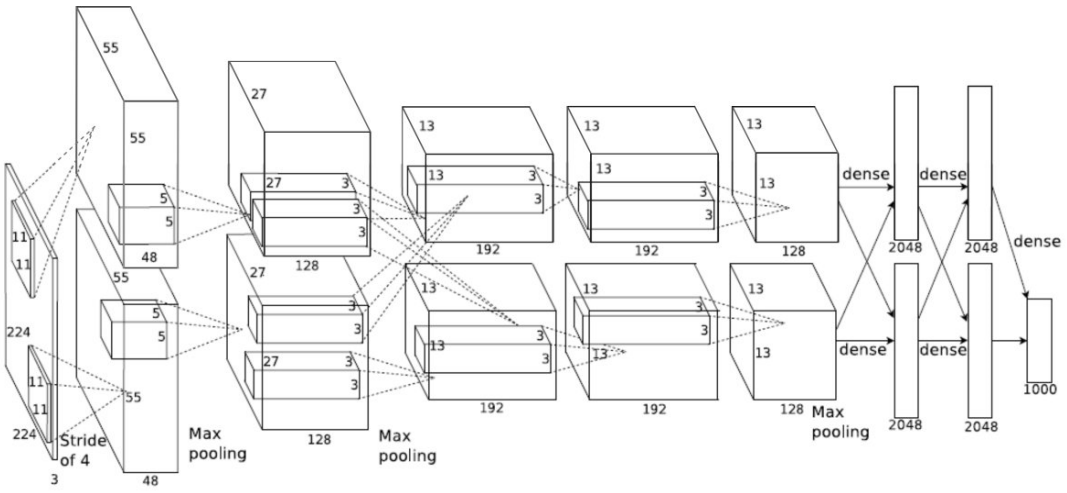

Figure 3.5 : AlexNet architecture.

extract the input's characteristics using local filters. These filters, referred to as kernels, utilize the spectral characteristics of image: only nearby pixels are related. Therefore, rather than linking each neuron to every neuron in the following layer, the knowledge is transmitted in so-called convolutions, which iteratively convolve around the image in a fixed-size window. The application that makes use of these small-sized kernels, including windows as small as 3x3 pixels, produces an extracted feature map that is capable of detecting simple features such as edges and shapes in previously concealed layers [51]. Standard CNN architectures, such as the one shown in Fig. 3.5, include a pooling layer and multiple convolutional layers. They serve a dual purpose: by pooling the image into a smaller size, the number of dimensions decreases significantly, resulting in an important decrease in computational time. Second, this pooling function enables the subsequent convolutions to examine information over a larger region of the image, which allows the interpretation of higher-level image characteristics.

Since the ANN structure is receptive to translation and shift deviation, the CNN has been developed as an extension of the ANN. CNN's architecture ensures translation and shift invariance. Fig. 3.6 illustrates a generic CNN network structure. It consists of convolution, pooling, and fully connected layers and is a feed-forward network. It is a deep neural network whose convolutional layers alternate with subsampling layers.

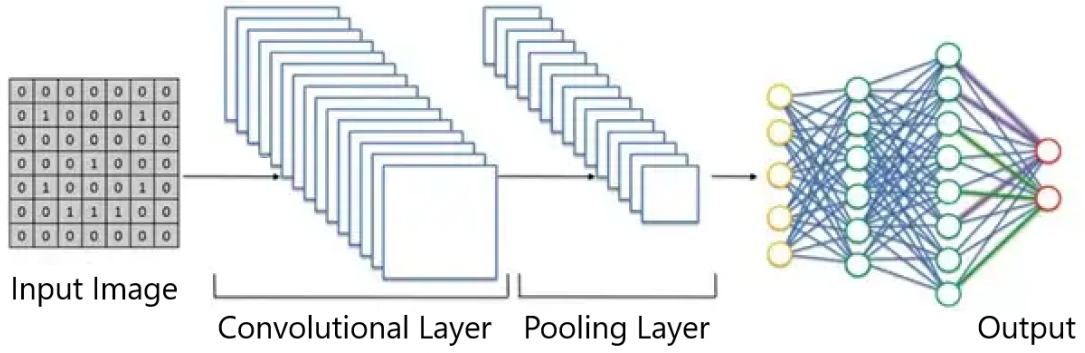

Figure 3.6 : Generic CNN structure.

CNN is best described in terms of its two steps: the alternating convolutional and subsampling stages and the classification stage. The convolution layer convolutes the input with a set of filters, like producing feature maps. These feature maps are further reduced by subsampling. The classification stage is then given the kernels or supervised features of the top convolution filters and subsampling.

With labeled source data, filters are fine-tuned to produce supervised features. CNNs are capable of ignoring minor positional variations, i.e., they seek patterns not only in a specific image position but also in moving patterns. In the field of medical image processing, deep learning techniques employed in recent years continue to demonstrate outstanding performance, as they do in many other domains [31]. Detection, segmentation, and classification of medical data are just a few areas where deep learning models have been successfully implemented. Using medical imaging methods like computed tomography (CT), magnetic resonance imaging (MRI), and X-rays, images and signals are analyzed using deep learning models. As a consequence of these analyses, diabetes, brain tumors, cancer of the skin, and cancer of the breast are easier to detect and diagnose [64,65].

Researchers encounter one of their greatest challenges when assessing and dealing with medical data in the restricted quantity of available datasets. Typically, the amount of medical data obtained from COPD patients is quite limited. At this point, deep transfer learning is the optimum solution [66].

3.3 Deep Transfer Learning

After providing a brief history of transfer learning, this section discusses its advantages, difficulties, and general strategies. Due to the vast amount of literature in this field as a result of decades of research, this thesis examines only a small portion of it. In order to better evaluate the findings of this thesis, we discuss the topics required to comprehend deep transfer learning approaches.

In recent years, artificial intelligence (AI) has made significant advances in a variety of fields, including computer vision, natural language processing, and robotics. Transfer learning, a subfield of artificial intelligence, has emerged as a successful approach for applying the knowledge of previously trained models to new tasks. This section examines the history, theory and applications of transfer learning in artificial intelligence. The objective of studying transfer learning is to develop intelligent systems that can learn and generalize effectively from limited labeled data. This issue is addressed by transfer learning, which improves performance on target tasks by employing knowledge acquired from related or previous tasks.The purpose of this section is to provide a thorough comprehension of transfer learning and its potential impact on AI research and applications.

In many knowledge engineering domains, such as classification, regression, and clustering, machine learning technologies have already attained significant success [67]. Nevertheless, many machine learning methods are only effective under the supposition that the training and test data come from the same distribution and feature space. When the distribution shifts, the majority statistical models must be reconstructed from scratch using newly gathered training data. In many real-world applications, retrieving the necessary training data and recreating the models is either prohibitively expensive or impossible, just like the situation we met in this research. It is desirable to reduce the effort and time required to retrieve training data. In such circumstances, knowledge transfer or transfer learning between task domains would be advantageous. It is necessary to train high-performance learners with data from multiple domains that is more readily accessible. In such instances, efficient knowledge transfer would significantly enhance the effectiveness of learning

by eliminating costly data-labeling efforts. Transfer learning has emerged in recent years as a new framework to resolve this issue. The transfer learning solutions are data-size-independent and applicable in settings with enormous data volumes [68].

The greatest benefit of transfer learning is that it enables training with fewer datasets at a lower cost. The model that needs to be trained gets the knowledge that the pre-trained model learned from an extensive dataset. A pre-trained model is a network that has been trained on a large benchmark dataset to solve a comparable problem to the one researchers wish to solve. Due to the computational expense of training such models, it is a standard strategy to import and employ models from published literature, as in the case of this thesis. Transfer learning tries to create a framework for leveraging previously learned information to tackle new problems that are similar to those previously encountered, more quickly and efficiently. Additionally, the pre-trained network can be retrained using the task-specific data by fine-tuning one or more of its layers. The distributions of the source and target problems may differ or be the same, as may the labels of the source and target problems. Both the source and target problems in this thesis have different distributions and labels.

3.3.1 Brief history

The research on the subject of transfer learning is motivated by the ability of individuals to logically apply previously acquired knowledge to solve brand-new problems swiftly or with better outcomes. The root cause for Transfer learning in the field of machine learning was addressed during an NIPS-95 workshop on "Learning to Learn" which focused on the demand for lifetime methods of machine learning that keep and reuse knowledge previously acquired.

Learning to learn, knowledge transfer, inductive transfer, lifelong learning, metalearning, context-sensitive learning, multitask learning, knowledge-based inductive bias, knowledge consolidation, and cumulative/incremental learning are some of the names that research on transfer learning has been given since 1995 [69]. The multitask learning framework [70], which aims to learn numerous tasks simultaneously even when they are dissimilar, is one of them and is strongly related to transfer learning.

Finding the common (latent) elements that can help each particular activity is a standard strategy for multitask learning.

The Information Processing Technology Office (IPTO) of the Defense Advanced Research Projects Agency (DARPA) announced a new mission of transfer learning in 2005 with the Broad Agency Announcement (BAA) 05-29: a system's ability to recognize and use information and abilities acquired during prior jobs to new ones. This definition of transfer learning states that it seeks to take the information from any number of source tasks and apply it to a target task. In comparison to multitask learning, transfer learning focuses on the target task rather than simultaneously learning the source and target tasks. In transfer learning, the roles of both the source and the target tasks are not anymore symmetrical.

Transfer learning has been utilized effectively in a variety of classification problems, such as image classification [71]–[73], software defect classification [74], text sentiment classification [75], human activity classification [76], and multi-language text classification [77]–[79].

3.3.2 Benefits of transfer learning

Transfer learning provides a number of benefits and advantages in machine learning, but it also presents a number of obstacles. In this subsection, these are investigated. When applying transfer learning in practice, it is vital to comprehend these benefits and challenges. To achieve optimal results, it is necessary to carefully consider the source-target task relationship, data availability, and appropriate techniques.

Improved performance: One of transfer learning's main benefits is that it can result in enhanced performance on the target task, particularly when there are few labeled examples of the target task. Transfer learning enables a model to generalize more effectively, make more accurate predictions, and learn more efficiently by leveraging knowledge from an associated source task or domain.

Reduced data requirements: Transfer learning can be extremely advantageous when labeled data are scarce or costly to acquire for the intended task. Rather than starting from scratch and collecting a large labeled dataset, transfer learning enables the model

to leverage the knowledge gained from a source task or domain, which can significantly reduce the amount of data required for training the target model.

Faster training: Training deep neural networks from scratch on massive datasets can be computationally demanding and time consuming. Using pre-trained models or learned representations as a starting point, transfer learning can accelerate the training process. This initialization gives the model a head start, and it solely needs to fine-tune or adjust its parameters to the target task, resulting in rapid convergence and reduced training time.

Generalization to new tasks: Transfer learning allows models to learn abstract representations and higher-level characteristics that capture general patterns across tasks or domains, thereby facilitating generalization to new tasks. This generalization capability enables the model to perform well on unexplored tasks or domains, even when the source and target tasks are not identical. Transfer learning facilitates the application of prior knowledge to new contexts.

3.3.3 Challenges of transfer learning

Transfer learning is a powerful machine learning technique, but it is not without its challenges. To overcome these obstacles, careful consideration must be given to the task, data, model architecture, and training procedure. It frequently requires experimenting with various approaches and methods to determine the optimal transfer learning strategy for a given scenario. Listed below are some typical obstacles to transfer learning:

Task and domain mismatch: Transfer learning is predicated on the existence of similarities or connections between the target and the source tasks or domains. If the tasks or domains are excessively distinct, transfer learning may be ineffective or even result in a decline in performance. Understanding the degree of similarity and choosing an appropriate transfer learning strategy become essential to overcoming this obstacle. Transfer learning is most effective when the source and target tasks have a degree of similarity. If the tasks are extremely dissimilar, it may be difficult to effectively

transfer knowledge. Finding source tasks that are pertinent to the target task can be challenging.

Dataset size: Transfer learning frequently necessitates a large amount of labeled data for the source task. If limited labeled data is available, the performance of the transfer learning model may suffer. Inadequate data can result in overfitting or inadequate generalization.

Dataset bias: If the data used to pre-train the model contains biases, those biases may be transferred to the target task. This can lead to skewed predictions or discriminatory performance in the target task. Addressing dataset biases requires meticulous preprocessing and data analysis.

Representation learning: Transfer learning is dependent on the acquisition of representations from the source task that can be applied to the target task. Nonetheless, it is not always obvious which representations are most advantageous for the intended task. Choosing the appropriate layers or features to transfer can be a challenging endeavor.

Fine-tuning and generalization: Following the implantation of the knowledge gained from the source task into the target task, it is essential to fine-tune the model for the target task. Finding the optimal balance between retaining acquired knowledge and adapting to the intended task can be difficult. If the fine-tuning process is not carefully managed, overfitting or underfitting on the target task can occur.

Negative transfer: Negative transfer occurs when the transferred knowledge blocks or negatively affects performance on the target task. This can occur if the source task contains information that is irrelevant or contradictory to the target task. Negative transfer can be mitigated through the careful selection of source and target domains and the application of suitable model adaptation techniques.

Computational resources: Transfer learning models, particularly those based on deep neural networks, can be computationally costly to train and necessitate substantial computing resources. Training on large datasets or utilizing complex architectures can be time-consuming and may necessitate the use of robust hardware.

Availability of pre-trained models or data: Transfer learning requires pre-trained models or datasets for the source task. While pre-trained models are readily accessible for common tasks such as image classification and natural language processing, they might not be available or useful for specific or specific tasks. In such situations, it can be difficult to create or acquire relevant pre-trained models or data sets.

Overfitting or underfitting: Transfer learning is the process of refining or adapting a previously-trained model to the target task. During the adaptation process, there is a chance of overfitting or underfitting the target data. To avoid these issues, it is essential to strike a balance between the transfer of knowledge from the source task and the acquisition of task-specific features on the target task.

Ethical considerations: If the source task data contains sensitive or private information, ethical considerations arise when transferring knowledge from the source task. Transfer learning necessitates the protection of data privacy and adherence to ethical guidelines.

3.3.4 Transfer learning approaches

Here, some of the most important techniques for transfer learning are explained. In accordance with the characteristics of the target and source tasks or domains, each type has unique strengths and applications. The appropriate transfer learning strategy is determined by the available data, task similarities, and the problem's resources and constraints.

Pre-trained model transfer: In this technique, a pre-trained model, usually trained on a large-scale dataset like ImageNet for tasks related to computer vision or a huge corpus for tasks related to natural language processing, is utilized as a launching point. The weights and learned representations of the pre-trained model are then adjusted or modified for a new target task or domain with limited labeled data. This form of transfer learning is common and effective in a variety of domains, as the pre-trained model has already acquired generic features that are applicable to a variety of tasks.

Feature extraction transfer: In feature extraction transfer, a pre-trained model is utilized as a fixed feature extractor. The initial layers of the pre-trained model are

utilized to extract features from the input data, which are then used to train an entirely novel classifier or model for the target task. The target model can benefit from the knowledge encoded in the features by exploiting the learned representations of the pre-trained model, which capture general patterns from a distinct but related domain. This method is especially beneficial when the labeled data for the target task are limited.

Fine-tuning transfer: Fine-tuning transfer expands the pre-trained model transfer by enabling the modification of both the higher-level and lower-level layers of the pre-trained model. Lower-level layers capture low-level characteristics, while higher-level layers capture task-specific characteristics. The transferred knowledge could be improved and adapted to the particulars of the target domain by refining the model on the target task. Fine-tuning is typically employed when the target task is comparable to the source task, but has distinct characteristics.

Domain adaptation: Domain adaptation involves transferring knowledge between domains that have distinct distributions, such as the source domain and the target domain. The objective is to reduce the disparity or shift in the distribution of data between the domains, allowing the model to generalize well on the target domain despite having been trained on the source domain. Various techniques, including adversarial training, importance weighting, and domain alignment methods, are used to align the feature distributions or to learn domain-invariant representations.

3.3.5 Motivation for Utilizing Transfer Learning

As previously stated, transfer learning is necessary when there is a lack of data for target training. This may be the result of the data being rare, costly to acquire and categorize, or inaccessible. Using extant datasets that are related to, but not identical to, transfer learning solutions become an appealing strategy with the proliferation of big data sources. Due to the limited number of subjects used to collect data in the target domain, transfer learning technique was employed in this thesis.

To train deep learning models efficiently, a large labeled dataset is frequently needed. Nevertheless, obtaining a sizable labeled dataset might be difficult or expensive in

many real-world circumstances. Transfer learning enables the use of pre-existing models that have been trained on large datasets to increase performance even with little labeled data available for the target job. Deep learning model training can be time-consuming and expensive in terms of computing. The original model, which has already been trained on a sizable dataset, gives a head start by collecting general properties and representations through the use of transfer learning. This conserves computational resources because only the final layers need to be adjusted or trained for the new task. Models that have been pre-trained are commonly trained on a range of large datasets, which enable them to learn broad features that are useful for a variety of tasks. Transfer learning enables the model to transfer its understanding and generalize well to the new task when confronted with a new task in a similar domain. This is especially helpful when there is an abundance of labeled data accessible in a related domain but little labeled data available for the target activity.

Besides, the pre-training phase of pre-trained models has already taught them how to represent data in meaningful ways. These representations capture the appropriate structures and patterns in the data, giving the model a better place to start when tackling the new task. Comparing transfer learning to building a model from scratch, faster convergence is made possible and could result in better performance.

Overall, the motivation behind using transfer learning is to leverage the knowledge and representations learned by pre-trained models to enhance the performance, reduce data requirements, save computational resources, and improve convergence when tackling new tasks or working with limited labeled data.

4. DEEP TRANSFER LEARNING ARCHITECTURE FOR COPD DETECTION

This chapter describes the proposed deep learning architecture, dataset, signal-to-image transformation methods, deep transfer learning structure, and experimental setup utilized in this thesis. For the purpose of finding a solution to the COPD detection problem, it is divided into five phases.

• Phase of data collection: ECG raw data from two groups of individuals were collected in the hospital. In total, 96 hours of uninterrupted data collection occurred over the course of several days.

• Data conversion phase: Using frequency analysis techniques, raw ECG signals are converted into frequency domain equivalent scalogram images that can be used as input for deep learning algorithms. Scalograms are designed to be compatible with the input size of CNNs so that they can be incorporated into CNN architectures.

• Phase of data preparation: Generating and preparing image data for use in distinct CNN structures (training, validation and test data)

• Transfer Learning phase: Adapting and analyzing the pre-trained networks and trained-from-scratch model for COPD detection problem.

• Evaluation phase: Evaluating the proposed system's results and performance.

4.1 System Design

In this thesis, a system is developed that uses easily accessible heart signals and the power of deep transfer learning to diagnose COPD. Without requiring an additional medical exam, the proposed system will determine whether the signal's owner has COPD and the severity of their condition. As described in Chapter 2, it is a well-studied and established fact that the ECG signal and COPD are correlated [2]. As a result of its interactions with all body organs, the ECG signal contains disease-related information. In order for deep learning techniques to detect disease signs in the ECG signal, the heart signals of the patients are divided into 16-second and 32-second segments

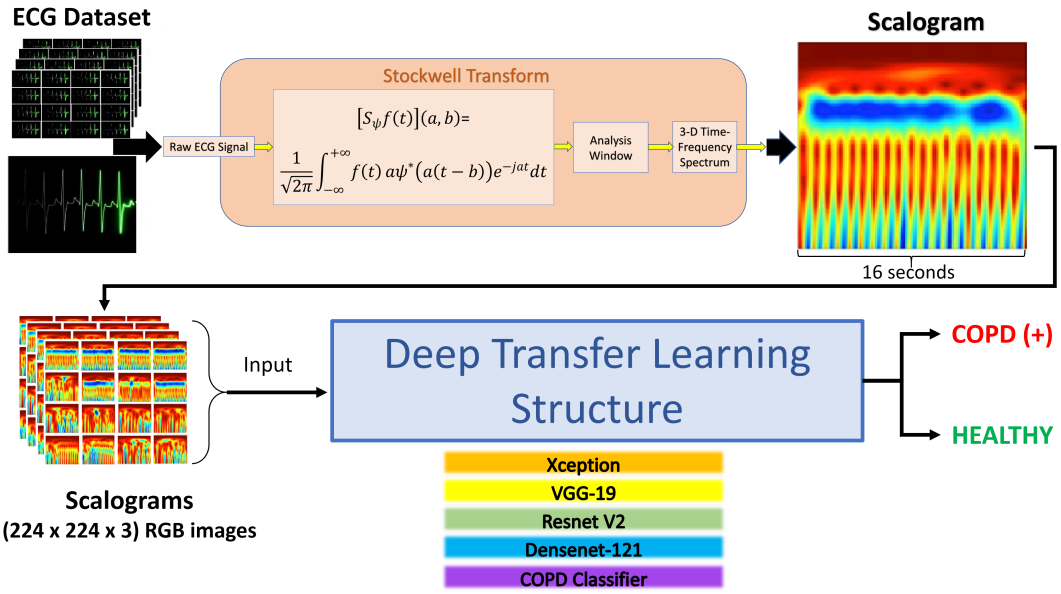

Figure 4.1 : Overview of the system design with Stockwell transform.

and converted to image format (224x224x3 RGB images) using signal frequency analysis techniques, the Wavelet Transform and the Stockwell Transform. Deep neural networks are fed this image dataset as input. Frequency analysis is utilized to improve the discrimination of the ECG signal's important signs. Fig. 4.1 and Fig.4.2 illustrate an overview of the proposed system design, which incorporates Stockwell and Wavelet Transforms.

4.2 Dataset Used

In the Sleeping Laboratory of Sakarya Hendek State Hospital, a chest diseases expert physician obtained ECG recordings of all of the subjects. Electrocardiograph SomnoScreen Plus PSG was utilized to record ECG signals at 256 Hz sampling rate. The device was regularly calibrated prior to each recording. In accordance with GOLD standards [65], chest diseases expert physician examined 12 subjects using a respiratory function test system and diagnosed each as "COPD" or "Healthy" after obtaining their medical records. Utilizing a Vitalograph Alpha spirometer, the respiratory function test was conducted.

The ECG signals obtained from two groups of individuals are utilized: six recordings from COPD patients and six recordings from healthy individuals. The duration of each

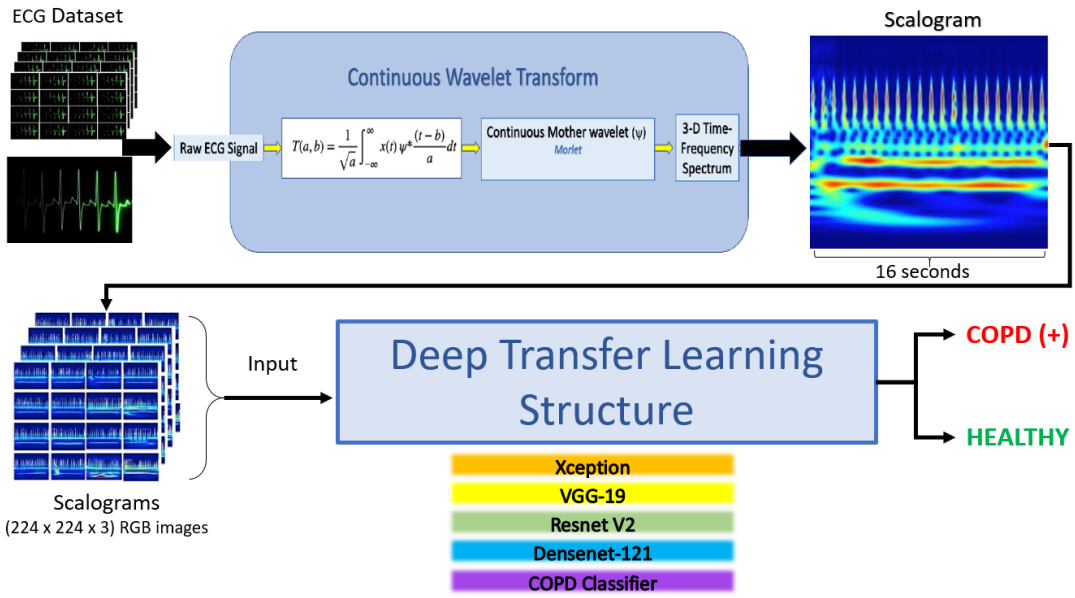

Figure 4.2 : Overview of the system design with wavelet transform.

subject's record is approximately eight hours without interruption. Six male subjects have been diagnosed with "COPD," while two female and four male subjects have been diagnosed with "Healthy" in the control group. During the consultations, all participants gave their informed consent for the use of their data. ECG signal data collected from the subjects is in 1-dimensional format: amplitude (millivolts, mV) vs. time (seconds, s). In Fig.4.3 and Fig.4.4, 4-second long representatives of two ECG categories are plotted.

After gathering the raw ECG data, Wavelet and Stockwell transform based time-frequency representations of the ECG signals, scalograms are created to be able to feed the deep neural networks with two-dimensional images. Scalograms are the absolute value of ECG signal's Continuous Wavelet Transform (CWT) and Stockwell Transform (ST) coefficients. Some ECG signal segments (16 seconds, 256 Hz) and their transformed equivalents (scalograms) for "COPD" and "Healthy" subjects are depicted in Fig. 4.5 and Fig. 4.6, respectively.

In Fig. 4.5, three distinct groups of area can be observed in the wavelet transform scalograms. In the upper portion of the Stockwell Transform scalogram, a yellow region indicates a frequency change intensity that is moderate. When compared to the

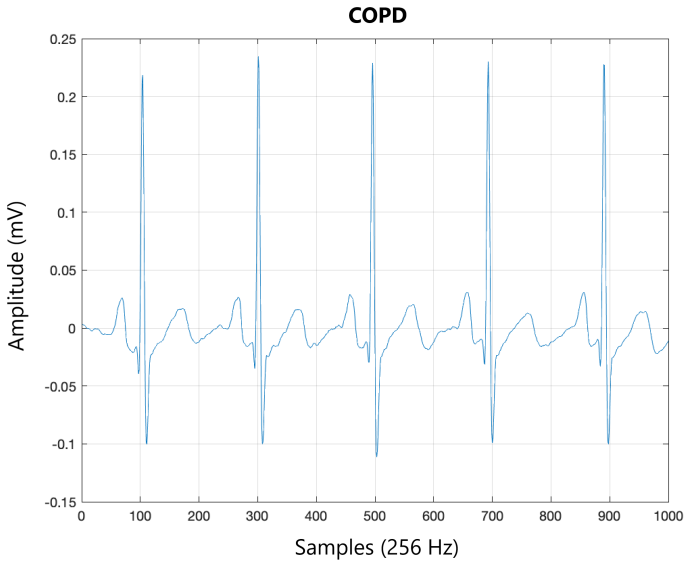

Figure 4.3 : ECG signal of a person with COPD, 4 seconds.

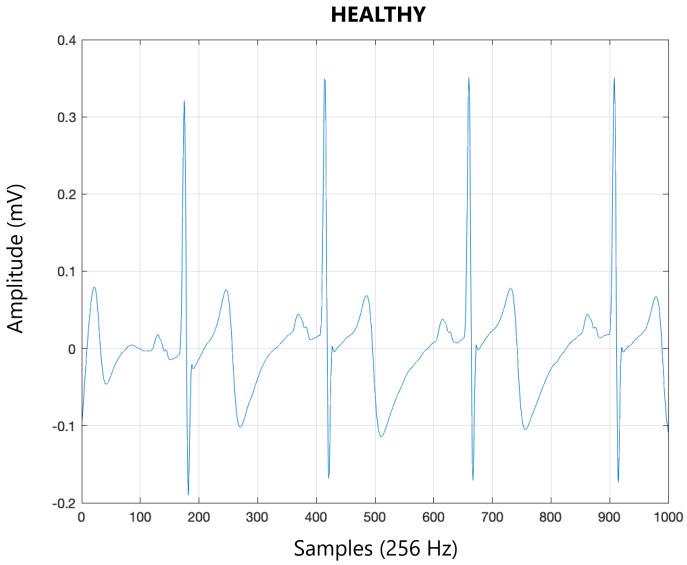

Figure 4.4 : ECG signal of a healthy person, 4 seconds.

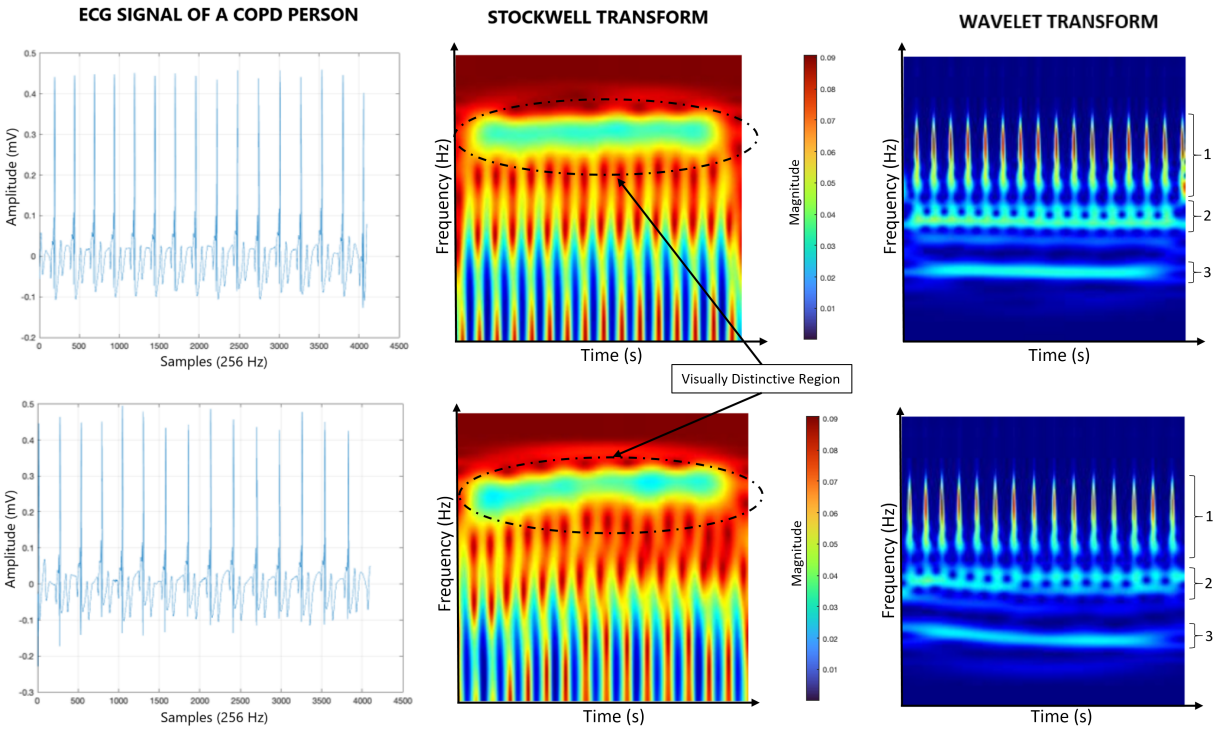

Figure 4.5 : A COPD person's ECG signal, Stockwell and wavelet scalograms.

next figure of a healthy person, these are the distinguishing signs of a COPD person's heart signal transformations.

In Fig. 4.6, observable in the wavelet transform scalograms is the addition of a new area as the fourth one. A blue region in the upper part of the Stockwell Transform scalogram indicates a low frequency change in intensity.

The periods chosen for the scalograms should contain sufficient R-peaks for locating the pattern's characteristics and be ones in which the features can be observed. In this context, 16 seconds and 32 seconds were selected as periods with medical significance, and it was determined that these periods would be suitable for experimental purposes. Consequently, two versions of the datasets are created. The ECG data of each subject is split into segments of 16 seconds (Dataset-A) and 32 seconds (Dataset-B) and categorized as "COPD" or "Healthy." The data quantities and labels for DataSet-A and DataSet-B are displayed in Table 4.1.

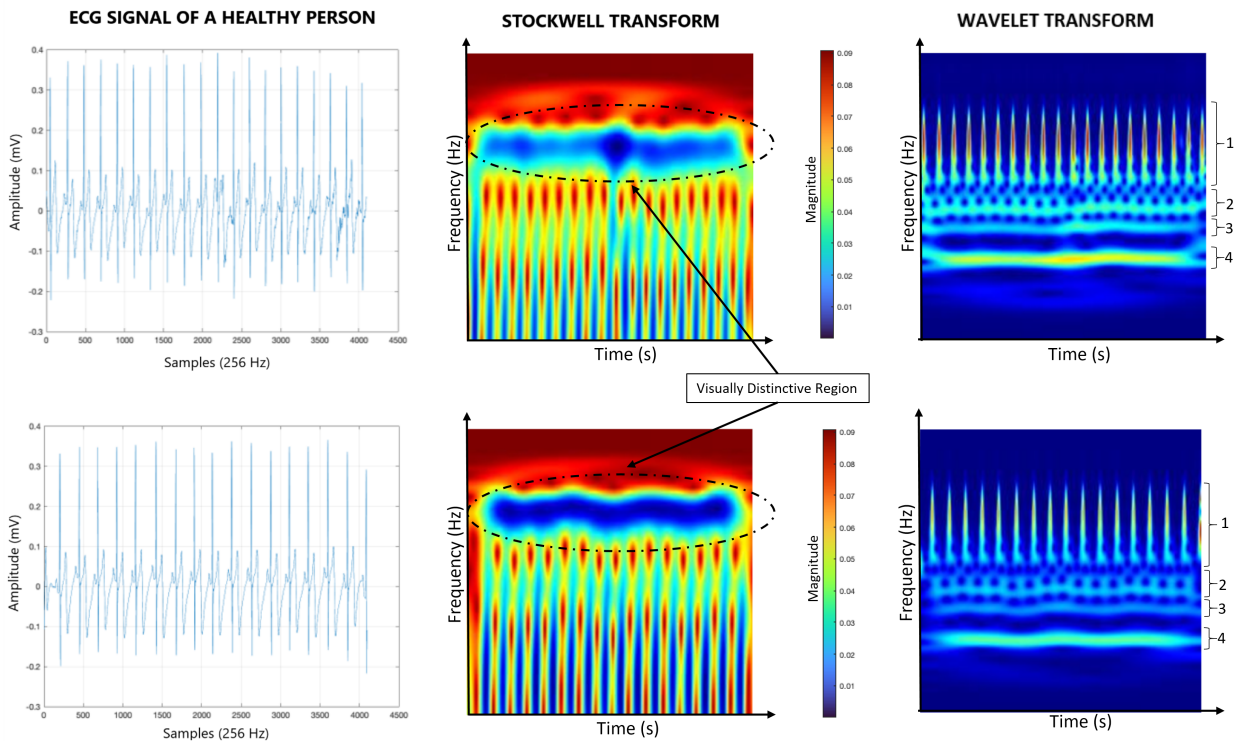

Figure 4.6 : A healthy person's ECG signal, Stockwell and wavelet scalograms.

Table 4.1 : Quantities of data labeled as "COPD" and "Healthy"

Dataset name	Epoch period	COPD labeled recordings	Healthy labeled recordings	Total quantity
DataSet-A	16 seconds	10906	10976	21882
DataSet-B	32 seconds	5453	5488	10941

4.3 Signal-to-Image Transform Methods

This section provides an overview of the signal to image transform and the methodology employed in this thesis. In the thesis, two well-established signal frequency analysis techniques are used to convert the ECG data of the subjects into an image format so that they can be utilized in the deep learning architecture. Since it has been hypothesized and investigated that the ECG signal itself carries the signs of COPD, it is essential to process and extract the signals for accurate classification.

Time-frequency analysis is typically employed to process local characteristics in non-stationary signal processing. Popular methods for feature extraction include the Short-Time Fourier Transform, Gabor Transform, Wigner-Ville distribution, Hilbert-Huang Transform, Wavelet Transform, and Stockwell Transform [80]. Despite their individual benefits, the majority of time-frequency representation techniques result in an unsatisfactory time-frequency distribution of non-stationary signals due to low resolution, cross-term interference, and other problems. In recent years, a number of signal processing techniques, such as the Continuous Wavelet Transform (CWT) and Stockwell transform, have been proposed to address these problems.

CWT: CWT is a mathematical technique employed for the analysis of the time-varying frequency characteristics of a signal. In contrast to the Fourier Transform, which offers frequency information across the entirety of a signal, the CWT enables the observation of variations in the frequency composition of a signal at different temporal instances.

Wavelet: A wavelet can be defined as a mathematical function that exhibits localization properties in both the time and frequency domains. The phenomenon under consideration involves a diminutive oscillation that can be displaced along a given signal in order to assess its degree of correspondence with the signal at various positions.

CWT coefficients: This term refers to the outcomes obtained through the application of the Continuous Wavelet Transform (CWT) on a given signal. The application of the CWT to an ECG signal involves the process of shifting the Morlet wavelet across the signal. This results in the computation of a measure of similarity, also known as

```
function convert_to_jpeg_WT(ECGData, Labels, parentFolder, childFolder)
    imageRoot = fullfile(parentFolder, childFolder);
    data = ECGData;
    labels = Labels;
    [~, signalLength] = size(data);
    fb = cwtfilterbank('SignalLength', signalLength, 'VoicesPerOctave', 12);
    r = size(data, 1);
    for ii = 1:r
        cfs = abs(fb.wt(data(ii, :)));
        im = ind2rgb(im2uint8(rescale(cfs)), jet(256));
        imgLoc = fullfile(imageRoot, char(labels(ii)));
        imFileName = strcat(char(labels(ii)), '\_', num2str(ii), '.jpg');
        imwrite(imresize(im, [224 224]), fullfile(imgLoc, imFileName));
    end
end
```

Figure 4.7 : Wavelet transform function code

correlation, at each location and for each available scale, which corresponds to the frequency of the wavelet. The CWT coefficients are obtained from the calculations conducted at various locations and scales. The presence of high CWT coefficients at a specific location and scale suggests the existence of a substantial frequency and location component within the signal. Conversely, low or close-to-zero CWT coefficients indicate a poor match between the wavelet and the signal at that particular location and scale. The CWT coefficients quantify the amplitude or intensity of distinct frequency constituents at different temporal locations within the signal. Subsequently, the aforementioned coefficients are employed to generate an image in which the colors are indicative of the magnitude of said coefficients. In brief, the utilization of CWT coefficients enables the examination of temporal variations in the frequency characteristics of an ECG signal. This analytical approach facilitates the identification and understanding of the underlying dynamics and patterns that characterize the signal.

Transform functions: This research employs a function named convert_to_jpeg_WT(), which accepts ECG signals (ECGData), corresponding labels (Labels), a parent folder path (parentFolder), and a child folder name (childFolder) as input parameters. The present function employs CWT method to convert ECG signals into visual representations, which are subsequently stored as output in the JPEG file format. The code implementation for the Wavelet transform function is presented in Fig. 4.7.

This function is responsible for generating the root path, denoted as imageRoot, which is utilized for the purpose of saving images. This is achieved by employing the fullfile function. The imageRoot is formed by combining the parentFolder and childFolder that are given as input. The cwtfilterbank() function is utilized for the purpose of generating a continuous wavelet filter bank. This filter bank is subsequently employed to process each individual row of the data matrix. Every individual row in the data matrix, denoted as ECGData, represents a distinct 16-second segment of the ECG signal.

The CWT coefficients are computed for individual segments of the ECG signal. Subsequently, these signal segments are transformed into RGB images using the ind2rgb() function. The color map employed in this study is the Jet color map. The image obtained, denoted as im, is subsequently resized to dimensions of 224x224 pixels using the imresize() function.

A file path, referred to as imgLoc, is generated using the label of the ECG signal. Similarly, a file name, denoted as imFileName, is created using the label and directory information. Subsequently, the resized image is stored at the designated location. The CWT coefficients are scaled to the range [0, 1] and subsequently converted to uint8 format using the function im2uint8 (rescale (cfs)). This processed data is then utilized to generate the RGB image.

The ind2rgb() function is employed for the purpose of transforming an indexed image into an RGB image. The indices of the CWT coefficients are taken into account and the ind2rgb() function is employed to produce an RGB image based on these indices. The input to the ind2rgb () function consists of a collection of indices. The resulting image from the ind2rgb () function is a representation where each index is substituted with its respective RGB color value derived from the color map. The images are stored in the JPEG format, with dimensions of 224x224 pixels. The filenames are generated based on their corresponding tags and directories.

The primary conversion function, convert_to_jpeg_WT (), requires a color map in order to associate indices with corresponding RGB values. The color map employed in this thesis for encoding purposes is the Jet color map, containing a total of 256 distinct colors. The Jet color map is widely utilized in the representation of data

with varying intensity or magnitude due to its alternating range of colors, making it a popular choice among researchers and practitioners. The color spectrum starts with a dark color of blue, followed by a sequential alternation between various intensities of green and yellow, ending in the final color of red. The selection of a color map holds significance as it influences the visual representation of the CWT coefficients within the RGB image. Various color maps possess the capability to highlight distinct characteristics of the data.

When generating an image, functions below are utilized:

im = ind2rgb (im2uint8 (rescale (cfs)), jet (256));

im : RGB image where the CWT coefficients are color mapped according to the Jet color map.

ind2rgb () : Converts uint8 indices to RGB values using the Jet color map.

im2uint8 () : Converts the scaled coefficients to uint8 format.

rescale (cfs) : Scales the CWT coefficients to the interval [0, 1].

Data loss during conversion: The conversion of CWT coefficients into an RGB image using the ind2rgb function may result in data loss, potentially leading to the loss of certain information contained within the signal. The reason for this is that we are converting a continuous range of values, specifically the CWT coefficients, into a discrete set of colors represented by RGB values.

Wavelet Transform has been utilized extensively for feature extraction. The Stockwell Transform is a technique for time-frequency spectral localization that combines Wavelet Transform and Short-Time Fourier Transform characteristics. In light of this context, the Wavelet Transform and Stockwell Transform are the preferred signal-to-image transformation methods for the proposed system. This thesis examines techniques for detecting COPD using images (scalograms) derived from the Wavelet Transform and the Stockwell Transform coefficients of ECG signals. To ensure compatibility with the employed CNN architectures, scalograms are generated as RGB images scaled to 224x224 pixels. Generative Adversarial Networks (GAN) or any other data augmentation methods were not used in this thesis because, as seen in Fig. 4.5 and Fig. 4.6, the distinctions between the two classes are not particularly clear, and

we did not wish to lose or obscure the distinguishing characteristics of the data through augmentation.

4.3.1 Wavelet transform

The Wavelet Transform (WT) technique is used to process ECG signals whose constituent frequencies vary over time. To efficiently classify ECG signals, a tool with high precision in both the frequency and time domains is required, allowing us to determine at what frequencies the signal oscillates and when these oscillations occur. The WT meets both of these conditions. WT is resistant to the noise in the signal. In addition, it is a tool that provides a representation of a signal by letting the translation and scale parameters of the wavelets vary continuously. The frequency domain properties of wavelets are used to design a filter bank in which each wavelet at increasingly larger scales (more dilated) passes a narrow, lower band of frequencies from the input signal.

Time domain procedure of the Wavelet Transform is to use wavelets of different scales, translate them over an interval along an input signal, and correlate the wavelet with the input at each of these scales and translations. Low-frequency components (longer period) are detected by larger scale wavelets, whereas higher-frequency components are detected by smaller scale wavelets [18]. This procedure generates a frequency-appropriate time resolution for each frequency. For slow oscillations, long epochs are utilized, while shorter epochs are used for faster oscillations. Due to the continuous nature of the ECG signal, this thesis employs the Continuous Wavelet Transform (CWT), a variant of WT for continuous signals.

When analyzing multiple signals in frequency vs. time, the filters are pre-computed once, and the filter bank is then passed as input to CWT for improved computational efficiency. Three parameters are used in that filter bank: signal frequency, signal length (sample size), and the wavelet bandpass filters per octave (voices per octave). The signal frequency is 256 Hz, with 4096 samples (256 Hz x 16 s) and 8192 samples (256 Hz x 32 s) for the signal length, and 12 voices per octave. In order to solve the problem of knowledge loss in the temporal domain, WT uses a time-localized oscillatory function as the mother wavelet. As the mother wavelet, the Morlet wavelet

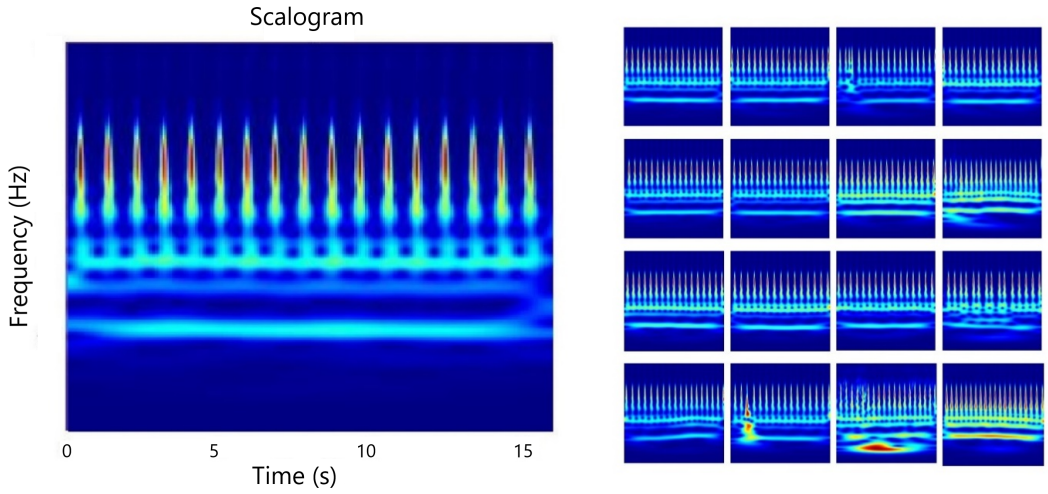

Figure 4.8 : Scalograms of ECG signals (wavelet transform)

is employed. The wavelets are visualized in time and frequency with the help of the filter bank. Fig. 4.8 depicts a scalogram of an ECG signal segment (16 seconds, 256 Hz) generated by the WT method, as well as 16 randomly selected samples from DataSet-A.

WT enables us to explore the frequency domain features of the ECG signal as an image by formatting the output as a scalogram image and then taking advantage of deep image classification techniques. Similar to the time-frequency domain, the CWT provides a description of a signal in the time-scale domain, enabling the representation of temporal properties at various resolutions at multiple resolutions. To do this, the signal is split up into scaled-down and time-transformed replicas of a prototype wavelet. Lower scales result in shorter, quicker wavelets, which are equal to broader, higher-frequency filters, whereas higher scales translate into long, slow wavelets, which are equivalent to narrow, low-frequency filters. CWT successfully strikes the perfect balance between time and frequency resolution: quick components are well defined in time but less so in frequency, whereas slow pace patterns show up with a high frequency resolution but a poor time resolution. Due to its intrinsic multi-resolution capabilities, CWT is quite effective at locating and displaying singularities, so it has been widely utilized in ECG analysis [81].

The combination of waveform shape and timing interval features is crucial for precise ECG classification. This is to be expected, as there are arrhythmic beats whose classification depends on timing properties rather than waveform shape. The WT has been shown to be an effective tool for isolating relevant waveform morphology properties from the noise, baseline drift, and amplitude variance of the original ECG signal [81,82]. It has been observed that groups using the downsampled WT of the ECG signal as their feature set, as opposed to the original waveform, have exhibited high classification accuracy. Using wavelet decomposition for classification also significantly reduces calculation time [83].

4.3.2 Stockwell transform

The Stockwell Transform (ST) is derived from the Continuous Wavelet Transform. By combining the advantages of Short-Time Fourier Transform (STFT) and WT, Stockwell et al. proposed it [84], which has attracted significant interest in a number of scientific and engineering fields, such as bioinformatics, biomedical imaging, optics, and signal processing. It stands out because it offers frequency dependent resolution while still having a clear connection to the Fourier spectrum. It employs a window whose width decreases with frequency and provides resolution that is frequency-dependent. This transformation includes both amplitude and phase spectrum information [85].

It is a technique that involves both STFT and WT but falls into a different category. Stockwell Transform provides notable results in property extraction in the presence of noise. This makes Stockwell transform suitable for accurate detection and classification of signal differences. It has an explicit physical interpretation and usefulness for medical applications. The time-frequency spectrum of the modulated signal is focused. This time-frequency analysis technique provides a three-dimensional graph of a signal in terms of its energy, or magnitude, over time and frequency [86]. The Stockwell transform stands out because it offers frequency dependent resolution while still having a clear connection to the Fourier spectrum. Additionally, it can be thought of as a phase-corrected WT, giving time-frequency analysis more precise information about the local properties of a signal. However, its signal analysis ability

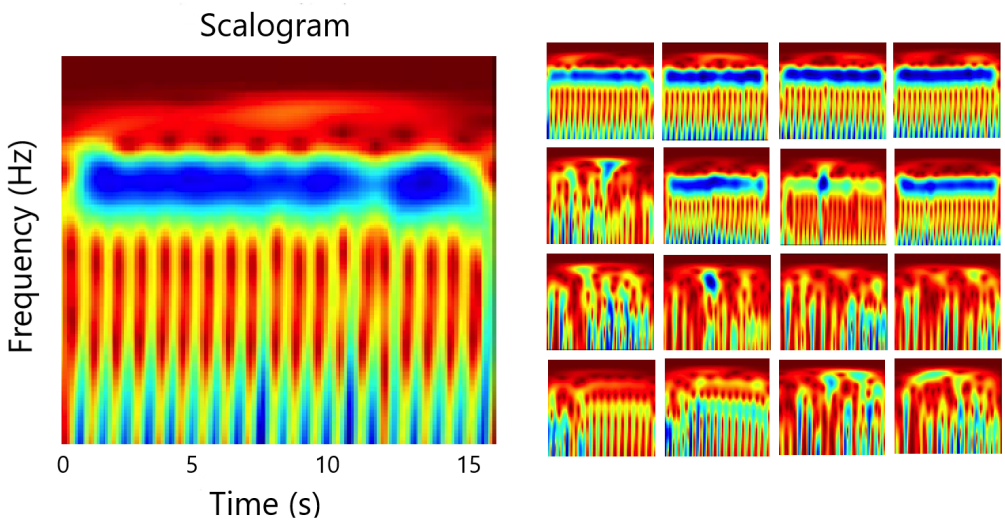

Figure 4.9 : Scalograms of ECG signals (Stockwell transform)

is restricted in the time-frequency plane [80] and this is observable in our experimental results. Experiments were conducted with the following parameters: a signal length of 16 or 32 seconds, a maximum frequency of 60 Hz, and a sampling frequency of 256 Hz. Fig. 4.9 shows a scalogram of an ECG signal (16 seconds, 256 Hz) generated by the ST technique and 16 randomly selected samples from DataSet-A.

4.4 Transfer Learning Strategy Used

COPD data is inherently difficult to collect from many people due to the nature of the problem. Therefore, we have limited participants for acquiring ECG signal data categorized as COPD positive or healthy. Deep transfer learning, which is known to be an appropriate approach for small sets of samples [24,34,87,88], is therefore considered to be employed in this thesis. Transfer learning is a methodology that makes use of the source-defined weights of the convolutional layers without retraining the network [12,87]. Employing a network loaded with pre-trained weights and then partially retraining it on the target task is required for fine-tuning. In the field of deep learning, fine-tuning a deep network is a usual method for learning both task-specific deep features and the methodology for discovering global features, such as general structures, present in every image. Typically, the fine-tuning technique permits more trainable weights at the highest level of the network since the convolutional layers at

the the highest of the network capture more abstract and high-level information than the initial layers, in which local features are learned. In the experiments, the effects of three main strategies are investigated: training from scratch, transfer learning, and transfer learning by fine tuning.

Using these strategies, it is shown how well the advanced CNN architectures for image classification work. A train-from-scratch strategy (named "COPD Detector" from this point on) is adopted by taking after well-known CNN architectures. The major techniques that CNNs employ for image classification are, training the CNN from scratch or re-purposing the pre-trained models, known as transfer learning [88] and fine-tuning [82]. While re-purposing the pre-trained models, the original classifier layers are replaced with new ones that fit the classification problem solved in this thesis. Five distinct CNN models are worked on according to each of the three transfer learning strategies below. A schematic representation of these strategies is shown in Fig. 4.10.

• Train the entire model: The architectures of the pre-trained models are used, and they are trained using DataSet-A. This is the training-from-scratch model, so the larger dataset on hand is used, and considerable computational power and time are expended for this strategy.

• Train some layers and leave the others frozen: A frozen layer means that it does not change during the training. As mentioned before, lower layers refer to general and problem-independent features, while higher layers refer to specific and problem-dependent features. Here, that dichotomy is played by choosing how much to adjust the weights of the network. Since DataSet-B contains a tiny quantity of data, more layers are kept frozen to avoid overfitting. In contrast, when the relatively larger DataSet-A is used, it is tried to improve the model by training more layers to the new task since overfitting is not an expected problem there. Both DataSet-A and DataSet-B are used in this strategy.

• Freeze the convolutional base: This case is an extreme example of the train/freeze trade-off. The fundamental idea is to maintain the convolutional base in its original state and then feed the classifier its outputs. Pre-trained models are employed as fixed feature extraction mechanisms, which is effective when the dataset is small or when

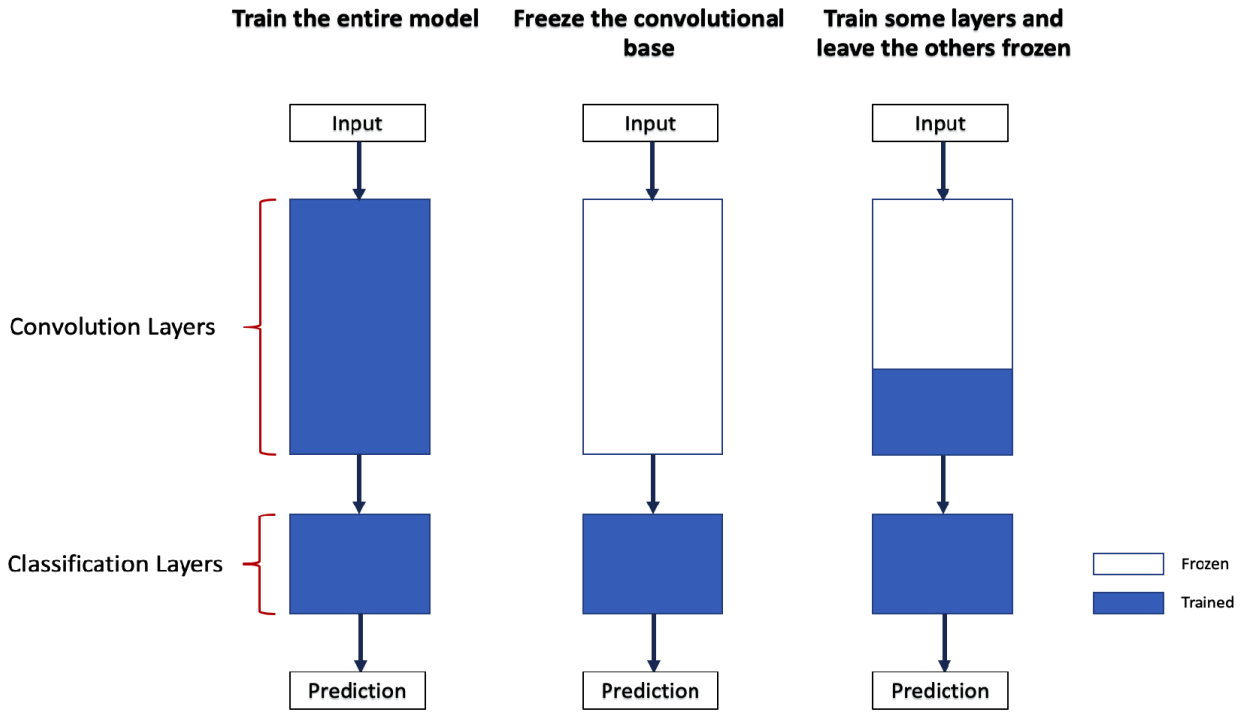

Figure 4.10 : Transfer learning and fine-tuning strategies

the pre-trained model solves a classification problem that is highly similar to the target classification problem, both of which are applicable to this thesis. Both DataSet-A and DataSet-B are used in this strategy.

5. EXPERIMENTAL RESULTS AND ANALYSIS

In this chapter, the outcomes of various training strategies and experimental setups are provided. Some explainable artificial intelligence (XAI) concepts and their usage in this thesis are also provided.

One important point should be made before delving into the experimental results. The best way to evaluate the effectiveness of the training is to have the network classify data it has never encountered. To maintain subject-independent validation results for each transfer learning model, cross-validation is used in this thesis. Cross-validation involves dividing data into training and validation sets, and then repeating this process multiple times with different splits of the data. This helps to provide a more robust estimate of how well a model generalizes to new data. 12-fold cross-validation was utilized in the training and testing procedures. During this step, the dataset is divided into 12 folds, with each fold including data for every subject. While 11 folds are used for training and validating the model, the last fold is concealed and is only used to evaluate the test set accuracy of the model. The procedure is repeated such that each fold serves as the test set. This approach increases the computational expense but improves the result's significance. The given results for accuracy in the tables are the averages of the values for accuracy at each fold.

For each transfer learning strategy, performance metrics including sensitivity, specificity, precision, F1 Score, validation accuracy, and test set accuracy are also reported to provide a clear and objective measurement of each strategy's effectiveness. To completely evaluate the effectiveness of the models, it is required to choose an appropriate evaluation index based on the below metrics. Regarding the classification task of the CNNs, the following metrics are recorded:

• correctly classified COPD signals: True Positives, TP

• incorrectly classified COPD signals: False Positives, FP

• correctly classified Healthy signals: True Negatives, TN

• incorrectly classified Healthy signals: False Negatives, FN

Sensitivity, specificity, precision, F1 score, validation accuracy, and test set accuracy values of the experiments are computed to evaluate the models. The sensitivity, also called recall, refers to how well a model detects stress among the true stress events. The specificity shows the ability of the experiment to correctly generate a negative result for people who don't have COPD. The precision represents the ratio of the number of true positives to the number of cases in which a model predicted stress. The F1 score represents the mean of sensitivity and precision. The primary metrics are test set accuracy and validation accuracy. When comparing models with very similar accuracy metrics, sensitivity, specificity, precision, and F1 score must all be taken into account because the comparison must be examined as a whole.

5.1 Experimental Setup

This thesis is conducted using a variety of CNNs, each of which utilizes a distinct learning strategy. All the experiments were performed via the Google Colaboratory Compute Engine infrastructure (TPU and GPU), utilizing the Python programming language, using Keras and TensorFlow as backends. Xception, VGG-19, InceptionResNetV2, DenseNet-121 and COPD Detector are employed for the ECG signal classification task. These deep CNNs used in this thesis were originally designed to classify images into 1000 categories. Here, it is preferred to leverage the performance of these four well-known CNNs that have been trained on large data sets for conceptually similar tasks. Three extra layers are added on top of these CNNs to reduce the number of classes from 1000 to 2, as there are only two classes involved in the COPD identification problem (COPD and Healthy). Dense (512), Dense (32), and Dense (2) are the three layers that have been added. The Table 5.1 provides a listing of the CNNs used and their primary specifications.

5.2 Hyperparameters Used

All the CNNs utilized in this thesis share certain hyperparameters in common. After a series of trials, it is attempted to balance the hyper-parameters to achieve the best

Table 5.1 : CNNs used in this thesis, and their basic specs.

CNN Name	Parameters	Depth	Input Size
InceptionResNetV2	55,873,736	572	(299, 299, 3)
Xception	22,910,480	126	(299, 299, 3)
VGG-19	143,667,240	26	(224, 224, 3)
DenseNet-121	8,062,504	428	(224, 224, 3)
COPD Detector	2,797,665	14	(224, 224, 3)

precision and accuracy. The CNNs were compiled using the "Adam" method of optimization. The learning rate is a hyper-parameter that controls how much the network's weights are modified. When using a pre-trained model, it is preferable to utilize a low learning rate because higher learning rates increase the danger of losing previous information. In the experiments, the learning rate is kept at 0.001. Choosing the proper number of epochs is also essential. Reducing the number of epochs results in under-fitting, whereas increasing the number of epochs leads to over-fitting. In the experiments, the training lasted between 5 and 40 epochs with a batch size of 32.

5.3 Limitations

It is necessary to acknowledge three limitations of this thesis. The first is that not all of the patients with COPD underwent diagnostic imaging such as chest computed tomography and echocardiography. Our physician (an expert in chest disease) diagnosed patients based on respiratory function tests and clinical history. These medical workups were also used to exclude patients who had heart diseases and lung diseases other than COPD. Second, since other conditions such as pericardial effusion could possibly affect QRS amplitude, to avoid confounding variables, patients with other conditions that could cause low QRS voltage are excluded. Consequently, the remaining 12 subjects' data are utilized for the thesis. The third limitation is that ECG data from six COPD patients and six healthy people is used, totaling 12 subjects. The recording period for each subject is 8 hours without interruption. Hence, a transfer learning strategy is used to compensate for the limited number of subjects. Further studies with large numbers of subjects with COPD are also being planned for experimentation in future work.

Table 5.2 : Train-the-entire-model strategy (10 epochs) with Stockwell transform.

CNN	Sensitivity	Specificity	Precision	F1 Score	Validation Accuracy	Test Set Accuracy
Xception	95.80%	97.60%	97.50%	96.60%	96.70%	96.70%
VGG-19	98.40%	79.80%	82.90%	90.00%	90.10%	89.10%
ResNetV2	97.20%	97.60%	97.50%	97.30%	97.10%	97.40%
DenseNet-121	94.40%	88.80%	89.30%	91.80%	93.00%	91.60%

Table 5.3 : Train-the-entire-model strategy (10 epochs) with wavelet transform.

CNN	Sensitivity	Specificity	Precision	F1 Score	Validation Accuracy	Test Set Accuracy
Xception	99.60%	98.60%	98.30%	98.90%	99.10%	99.90%
VGG-19	100%	0%	50.00%	66.66%	50.00%	50.00%
ResNetV2	99.80%	86.90%	85.60%	92.10%	92.50%	85.50%
DenseNet-121	94.80%	99.50%	99.40%	97.20%	97.60%	90.20%

5.4 Train-the-Entire-Model Strategy

All layers of the four distinct networks are trained with signal-to-image transformed ECG data (scalograms), adapting only their input and output parameters. Training all of the layers requires a significant amount of GPU/TPU resources and time. Performance metrics of this strategy are given for the input data transformed by ST in Table 5.2, and for the input data transformed by WT in Table 5.3. Observations indicate that the strategy is effective at classifying COPD and healthy signals. Unexpectedly, the VGG-19 model categorized all test set data as healthy when fed WT data as input. This unacceptable scenario has been investigated, and it will also be covered under the subsection titled Train Some Layers and Leave the Others Frozen. To give a hint, there are five convolutional blocks in VGG-19, and when more than three of them are trained, classification becomes problematic. Consequently, the Xception model trained with WT data and the InceptionResNetV2 model trained with ST data appear to outperform other models.

5.5 Fine-Tuning Strategy

Fine-tuning of a convolutional network is a process that must be continuously enhanced and maintained. As a starting point in this thesis, two fine-tuning sub-strategies are examined in the direction of the proposed strategy. "Freezing the convolutional base"

Table 5.4 : Freezing the convolutional base strategy (10 epochs) with ST.

CNN	Sensitivity	Specificity	Precision	F1 Score	Validation Accuracy	Test Set Accuracy
Xception	94.40%	90.60%	90.90%	92.60%	93.20%	92.50%
VGG-19	85.60%	99.00%	98.80%	91.70%	92.50%	92.30%
ResNetV2	86.40%	85.00%	85.20%	85.80%	85.70%	85.70%
DenseNet-121	89.20%	90.40%	90.20%	89.70%	90.85%	89.80%

Table 5.5 : Freezing the convolutional base strategy (10 epochs) with WT.

CNN	Sensitivity	Specificity	Precision	F1 Score	Validation Accuracy	Test Set Accuracy
Xception	98.60%	74.60%	75.10%	85.20%	85.10%	91.30%
VGG-19	95.20%	99.30%	99.10%	97.10%	97.50%	97.40%
ResNetV2	85.90%	77.10%	74.50%	79.80%	81.00%	79.20%
DenseNet-121	74.50%	99.60%	99.30%	85.10%	88.60%	88.40%

and "Training only a subset of layers while leaving the rest frozen" sub-strategies will be explained and investigated in this part.

5.5.1 Freezing the convolutional base

As its name suggests, the convolutional bases of the pre-trained networks are frozen and just the top classification layers of each network are trained with signal-to-image transformed ECG data. The term frozen here refers to the layers/convolution blocks remaining exactly as they were in their original state. The computational cost (GPU usage and processing time) is lower in comparison to the Train-the-Entire-Model Strategy because not all of the layers are trained from scratch. Based on Table 5.4 and 5.5, the results of this strategy are likely to succeed, but inferior to those of the first strategy. Although the performance degradation in InceptionResNetV2 is noticeable when both ST and WT are used, the best performer in this substrategy is VGG-19 which uses WT data as its input and has 97.40% test set accuracy and 97.50% validation accuracy.

5.5.2 Training some layers and leave the others frozen

In that sub-strategy, some layers are getting trained, including the top and experimentally selected ones below the top, the others are left frozen. The VGG-19

structure, which has the highest score of the previous sub-strategy, is worked on in this sub-strategy with the WT data as its input. Several fine-tuning modifications are examined in this particular subsection to get the best results. For example, it is investigated how it affects the classification results if the convolution blocks of the VGG-19 structure are made trainable in a certain order. In Table 5.6, each experimental instance is defined by a number that represents the number of trainable convolution blocks used in the experiment. As an example, CNN stated as "Fine-Tuning 3" refers to three convolution blocks made trainable beginning at the top of the CNN, but all the other layers were left frozen. Performance metrics for this sub-strategy are given in Table 5.6. As shown in the table, as the number of convolution blocks increases, accuracy and other performance metrics also improve. When only one convolution block is trainable, validation and test set accuracies are 97.00% and 97.80%, respectively; when three blocks are trainable, they are 98.90% and 99.10%. However, there is a saturation point. Since the VGG-19 network has a total of five convolutional blocks, it is anticipated that the network's performance will be comparable to the VGG-19 train-the-entire-model strategy when four blocks are made trainable. When we attempted it, we achieved the expected outcomes. The results of Fine-Tuning 4 were unsatisfactory as VGG-19 train-the-entire-model strategy. Consequently, Fine-Tuning 3 model has the best performance metrics in this strategy.

Table 5.6 : Training some layers and leave the others frozen strategy (10 epochs) with wavelet transform

VGG-19	Sensitivity	Specificity	Precision	F1 Score	Validation Accuracy	Test Set Accuracy
Fine-Tuning-1	95.30%	98.40%	97.80%	96.60%	97.00%	97.80%
Fine-Tuning-2	96.20%	96.90%	96.00%	96.10%	96.60%	98.70%
Fine-Tuning-3	98.60%	99.20%	98.90%	98.80%	98.90%	99.10%
Fine-Tuning-4	100%	0%	50.00%	66.66%	50.00%	50.00%

5.6 Customized Network, Training-from-Scratch Strategy

In addition to well-known and pre-trained CNN structures, one of the objectives of this thesis is to create a CNN structure with high performance in order to solve the COPD detection problem. Using as an example the VGG-19 structure that was relatively more effective in the previous experiments, a customized CNN structure was created and named "COPD Detector" in this sub-strategy. The general convolution layer structure of this custom network was inspired by VGG-19, and since Fine Tuning-3 produced the best results, we decided to use a structure with three convolution blocks. Network structure of COPD Detector is shown in Table 5.7.

Table 5.7 : Network structure of the COPD Detector

Conv2D	(32,(3,3)) input shape= (224,224,3)
Activation	Relu
MaxPooling2D	Pool Size= (2,2)
Conv2D	(32,(3,3))
Activation	Relu
MaxPooling2D	Pool Size= (2,2)
Conv2D	(64,(3,3))
Activation	Relu
MaxPooling2D	Pool Size= (2,2)
Flatten	
Dense	64
Activation	Relu
Dropout	0.5
Dense	1
Activation	Sigmoid

Table 5.8 : COPD detector for different epoch values with Stockwell transform.

COPD Detector	Sensitivity	Specificity	Precision	F1 Score	Validation Accuracy	Test Set Accuracy
5 epochs	90.00%	94.10%	94.10%	92.00%	92.00%	90.50%
10 epochs	90.30%	92.00%	92.20%	91.20%	91.10%	90.50%
15 epochs	86.60%	93.70%	93.50%	89.90%	90.00%	89.60%
20 epochs	92.10%	90.30%	94.00%	92.10%	91.90%	91.00%
25 epochs	92.30%	91.50%	91.90%	92.10%	91.90%	90.50%
30 epochs	93.60%	92.40%	92.80%	93.20%	93.00%	90.90%
35 epochs	93.10%	87.60%	88.70%	90.90%	90.40%	90.40%

Table 5.9 : COPD detector for different epoch values with wavelet transform.

COPD Detector	Sensitivity	Specificity	Precision	F1 Score	Validation Accuracy	Test Set Accuracy
5 epochs	97.70%	21.80%	49.30%	65.50%	55.00%	89.90%
10 epochs	94.70%	97.20%	96.30%	95.50%	96.10%	96.10%
15 epochs	97.90%	94.50%	93.30%	95.50%	96.00%	98.50%
20 epochs	87.00%	95.30%	93.50%	90.10%	91.60%	92.70%
25 epochs	96.40%	96.60%	95.70%	96.00%	96.50%	97.30%
30 epochs	93.80%	97.30%	96.40%	95.10%	95.80%	97.50%
35 epochs	96.50%	97.60%	96.90%	96.70%	97.10%	97.30%

COPD Detector is trained from scratch for multiple epochs, utilizing scalograms generated using both the ST and WT. Table 5.8 and 5.9 display the performance metrics for this sub-strategy for ST and WT, respectively. The COPD Detector is observed to compete with the other strategies in every metric, achieving outstanding accuracy for a variety of epoch values. However, when the experiments are examined separately, it can be seen that using WT data is more efficient than using ST data in terms of classification performances. In terms of test set and validation set accuracy values, the 15, 25, and 35 epoch runs using WT data as input generate the highest-quality classification results.

5.7 Cross-Validation Results

Validation is an essential step in evaluating any deep learning model's robustness and performance. The commonly used method of cross-validation provides a thorough way to assess the generalizability and effectiveness of a model. This section presents and analyzes the cross-validation results of the approach presented to detect COPD

from ECG signal. This section, which made use of one of the models we have used before, aimed to ensure appropriate representation and evaluation of the predictive power of the method by thoroughly analyzing its performance over a range of folds. The cross-validation analysis's result is crucial in confirming the validity and dependability of our suggested methodology and illuminating its possible applicability and resilience in COPD detection from ECG signals. This subsection also provides a comprehensive analysis of the cross-validation metrics and results in order to elucidate the performance insights obtained and their implications with regards to the effectiveness of the proposed methodology.

Table 5.10 shows the outcomes of each iteration, in which only one healthy person and one COPD patient were excluded from the training process out of a total of 12 subjects, which included 6 COPD patients and 6 healthy people. From-scratch trained Xception model was utilized, running one epoch for each experiment on the 16-second dataset generated via the Stockwell transform.

Based on the outcomes of the cross-validation process, the employed methodology demonstrates efficacy and reliability. The robustness and generalization capacity of the model are validated by the outcomes attained in each iteration, in which only one person with COPD and one healthy person were left out of the training process. Based on the validation and testset accuracy results, the obtained results validate the model's ability to detect COPD in a heart signal. This observation indicates that the suggested methodology has the potential to succeed in this field. This research emphasizes the applicability and overall performance of the proposed approach while providing a foundation for future investigations.

5.8 Comparative Analysis of the Results

The results suggest that entirely trained Xception model, fine-tuned VGG-19 models, and COPD Detector model that trained for 15 epochs, achieve the best performance metrics over the rest of the CNNs. Since the dataset used in these experiments is balanced, meaning that each class is represented by an equal amount of data, and the majority of CNNs appear to perform well in terms of accuracy, sensitivity, specificity, precision, and F1 score as a whole, evaluation can be considered to have led to

Table 5.10 : Cross validation results for each subject with Stockwell transform.

Subjects Excluded for Testset	Validation Accuracy	Test Set Accuracy
1st COPD patient and 1st HEALTHY subject Out	95.17%	88.25%
1st COPD patient and 2nd HEALTHY subject Out	95.55%	83.94%
1st COPD patient and 3rd HEALTHY subject Out	98.30%	91.50%
1st COPD patient and 4th HEALTHY subject Out	99.05%	93.69%
1st COPD patient and 5th HEALTHY subject Out	98.36%	97.25%
1st COPD patient and 6th HEALTHY subject Out	94.84%	93.12%
2nd COPD patient and 1st HEALTHY subject Out	94.54%	88.69%
2nd COPD patient and 2nd HEALTHY subject Out	98.21%	86.44%
2nd COPD patient and 3rd HEALTHY subject Out	94.74%	92.31%
2nd COPD patient and 4th HEALTHY subject Out	94.33%	90.81%
2nd COPD patient and 5th HEALTHY subject Out	94.55%	91.69%
2nd COPD patient and 6th HEALTHY subject Out	97.90%	91.56%
3rd COPD patient and 1st HEALTHY subject Out	94.69%	95.31%
3rd COPD patient and 2nd HEALTHY subject Out	98.16%	92.81%
3rd COPD patient and 3rd HEALTHY subject Out	94.23%	97.50%
3rd COPD patient and 4th HEALTHY subject Out	94.05%	96.81%
3rd COPD patient and 5th HEALTHY subject Out	98.03%	98.00%
3rd COPD patient and 6th HEALTHY subject Out	94.10%	97.25%
4th COPD patient and 1st HEALTHY subject Out	94.57%	90.81%
4th COPD patient and 2nd HEALTHY subject Out	95.04%	72.94%
4th COPD patient and 3rd HEALTHY subject Out	97.59%	98.25%
4th COPD patient and 4th HEALTHY subject Out	94.25%	92.25%
4th COPD patient and 5th HEALTHY subject Out	97.25%	93.99%
4th COPD patient and 6th HEALTHY subject Out	97.25%	94.38%
5th COPD patient and 1st HEALTHY subject Out	94.61%	92.37%
5th COPD patient and 2nd HEALTHY subject Out	95.45%	73.06%
5th COPD patient and 3rd HEALTHY subject Out	94.39%	96.50%
5th COPD patient and 4th HEALTHY subject Out	94.74%	94.63%
5th COPD patient and 5th HEALTHY subject Out	93.74%	97.37%
5th COPD patient and 6th HEALTHY subject Out	96.81%	94.13%
6th COPD patient and 1st HEALTHY subject Out	94.76%	91.94%
6th COPD patient and 2nd HEALTHY subject Out	95.49%	76.19%
6th COPD patient and 3rd HEALTHY subject Out	94.56%	97.12%
6th COPD patient and 4th HEALTHY subject Out	94.60%	94.44%
6th COPD patient and 5th HEALTHY subject Out	94.49%	94.13%
6th COPD patient and 6th HEALTHY subject Out	94.29%	92.56%
Average	95.63%	91.78%

Table 5.11 : Accuracy values of the best three CNNs

CNN	Strategy	Validation Accuracy	Test Set Accuracy
Xception	Train the Entire Model	99.10%	99.90%
VGG-19	Fine-Tuning-3	98.90%	99.10%
COPD Detector	Trained-from-Scratch (35 epochs)	97.10%	97.30%

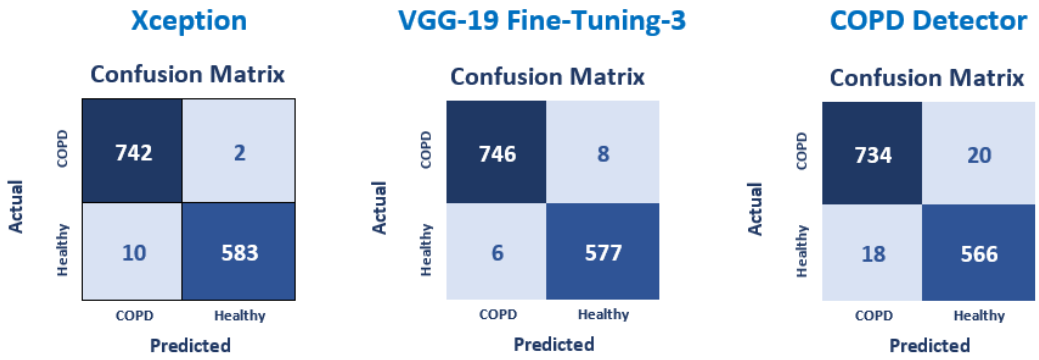

Figure 5.1 : Confusion matrices of the best three CNNs

accurate conclusions. Using the combination of accuracy, sensitivity, and specificity as the criterion for selecting the top three models, the fully trained Xception model, the fine-tuned VGG-19 model, and the COPD Detector (trained from scratch for 15 epochs) stand out. In order to further assess these leading models, confusion matrices and accuracy values are shown in Table 5.11 and Fig. 5.1, respectively.

The best performance is obtained with a test set accuracy of 99.9%, a sensitivity value of 99.6%, and a specificity value of 98% for the Xception model, which is trained entirely with WT data as input. The Xception model provides superiority over the other 2 models in both the training and testing stages. The experimental evaluation also showed that the deep transfer learning structures provided over a 5 percentage point improvement over our previous study, a rule-based decision tree model with 93.89 percent accuracy. Thirty-four separate experiments investigating various approaches were conducted for this thesis, with 12 of them yielding better results than the prior decision tree model. It must be noted that, in the majority of experimental investigations for each model, it appears that using WT data as input

yields better results than using ST data.

5.9 Explainable AI Projection of the Research

Even though machine learning and deep learning produce accurate predictions, critics of these techniques have claimed that scientists are building "black box" models. But today that is a false impression. Using Explainable Artificial Intelligence (XAI) methods, it is now possible to interpret models from deep learning and machine learning. Infact, model interpretation is a very active area for both academic and industrial researchers. Interpretability is the extent to which a person can reliably predict the outcomes of an ML model or comprehend the reasons behind a decision.

Explainability has recently become a critical topic in deep learning because it is difficult to provide understandable explanations of the inner workings and decision-making mechanisms of deep learning algorithms, despite the fact that deep learning algorithms have demonstrated remarkable performance on various tasks. Also, there are numerous ways in which a model or its evaluation could be flawed.

Even in highly regulated industries like medicine and finance, more businesses are now successfully utilizing machine learning and deep learning in their decision-making processes or have plans to do so in the future due to their interpretability.

Since the utilization of deep learning also necessitates a certain level of general trust in the model, well-known XAI methodologies such as the Local Interpretable Model-Agnostic Explanations (LIME) by Ribeiro et al. [89], and the SHapley Additive exPlanations (SHAP) by Lundberg et al. [90] are used to examine the explainability of our research.

5.9.1 Local interpretable model-agnostic explanations (LIME)

LIME functions by fitting a local, simpler model to the instance that needs to be explained. By collecting samples surrounding the instance to be explained, a new dataset is generated. It employs a kernel function to weight the significance of each instance of the new dataset based on the explained occurrence's location. Using

the new dataset, the expected classes for the new dataset, and the weights, it fits a weighted linear model. This linear model is utilized to provide an explanation for the prediction. This subsection describes four randomly selected scalogram images (COPD_3604, COPD_3610, HEALTHY_6185, HEALTHY_6178) and their classification explanations using the fine-tuned VGG-19 model and the LIME method.

In Figures 5.2, 5.3, 5.4, and 5.5, explanation files of four different scalogram images that are classified as COPD or Healthy are presented. In addition to the original scalogram image (a), there are three additional representations in the figures: the top five zones that influence the classification result only positively (b), the top five zones that influence the classification result both positively and negatively (c), and the heatmap of the entire scalogram (d). In the heatmaps, the locations of the so-called superpixel regions that influence the classification result in positive and negative directions, are colored blue and red, respectively. On the heatmaps, concentrations of both classes are visible in specific regions.

Regarding the used parameters, if positive_only is true, only pixels that positively affect the classification are displayed. False shows both positive and negative effects on the scalograms. The num_features parameter specifies the maximum number of fields that have the greatest influence on the classification. If the hide_rest parameter is true, only the regions specified by num_features and positive_only are displayed and the remainder of the image is hidden.

When the explanations are analyzed, it can be seen that the parts of the images that have a positive effect on the classification result are in mostly similar areas. In the COPD images without breaks and scatter, the classification was correct with high accuracy, and the pixels in the upper middle and middle right parts of the images were more effective in determining the result.

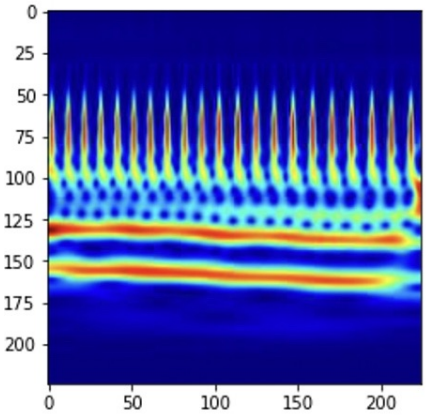

(a)

COPD_3604
224 x 224 RGB Scalogram

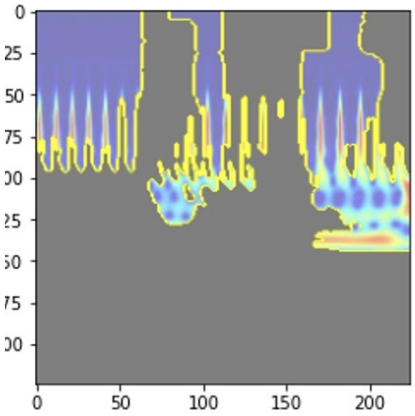

(b)

positive_only = True
num_features = 5
hide_rest = True

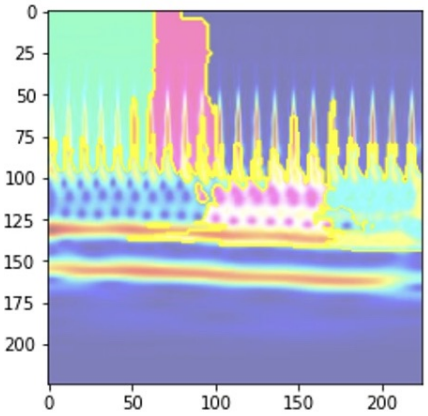

(c)

positive_only = False
num_features = 5
hide_rest = False

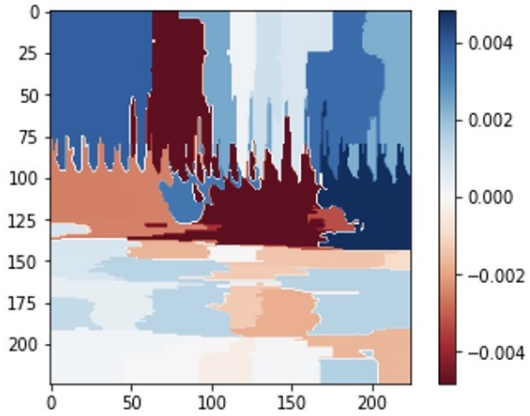

(d)

Mapping each explanation weight
to the corresponding superpixel

Figure 5.2 : LIME explanations: ECG of a person with COPD, correctly classified as COPD with 99,9 % probability

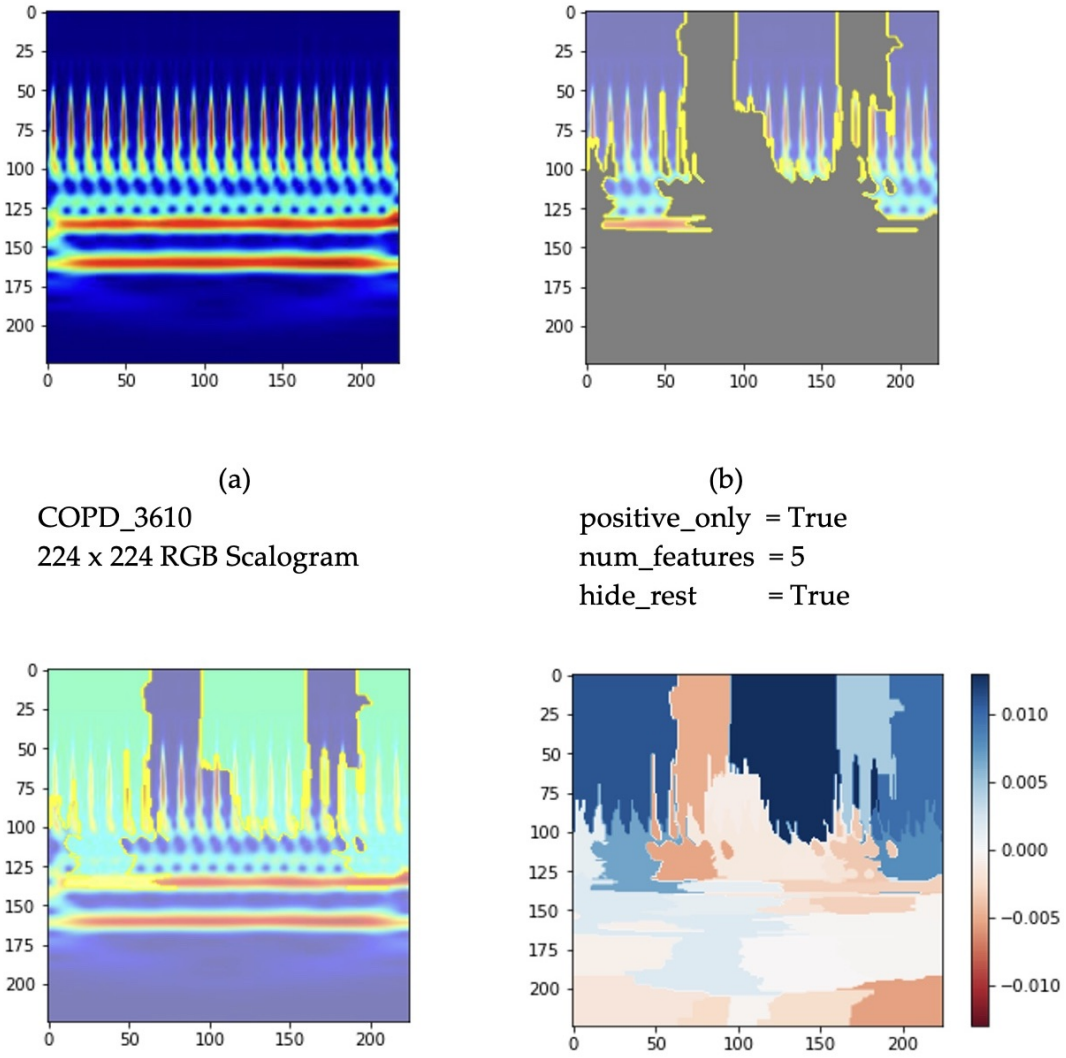

Figure 5.3 : LIME explanations: ECG of a person with COPD, correctly classified as COPD with 99,7 % probability

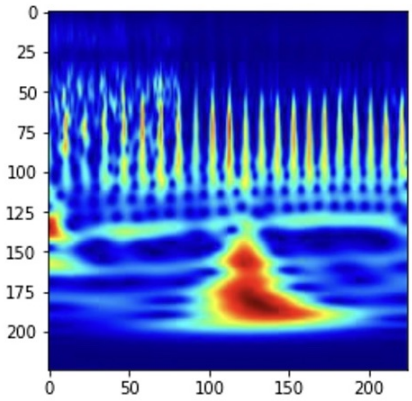

(a)
HEALTHY_6185
224 x 224 RGB Scalogram

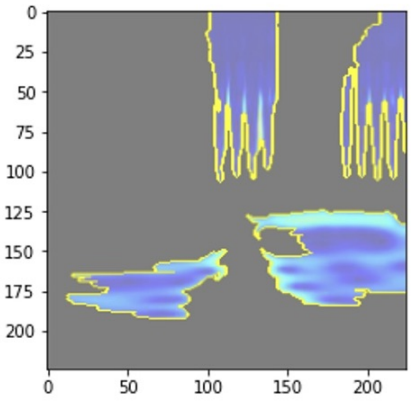

(b)
positive_only = True
num_features = 5
hide_rest = True

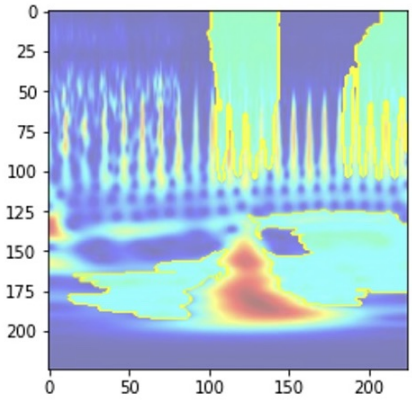

(c)
positive_only = False
num_features = 5
hide_rest = False

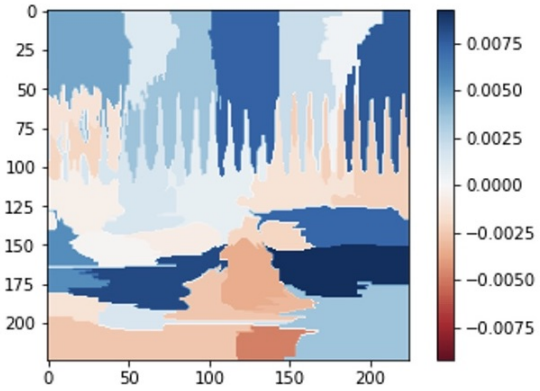

(d)
Mapping each explanation weight
to the corresponding superpixel

Figure 5.4 : LIME explanations: ECG of a healthy person, correctly classified as HEALTHY with 79,1 % probability

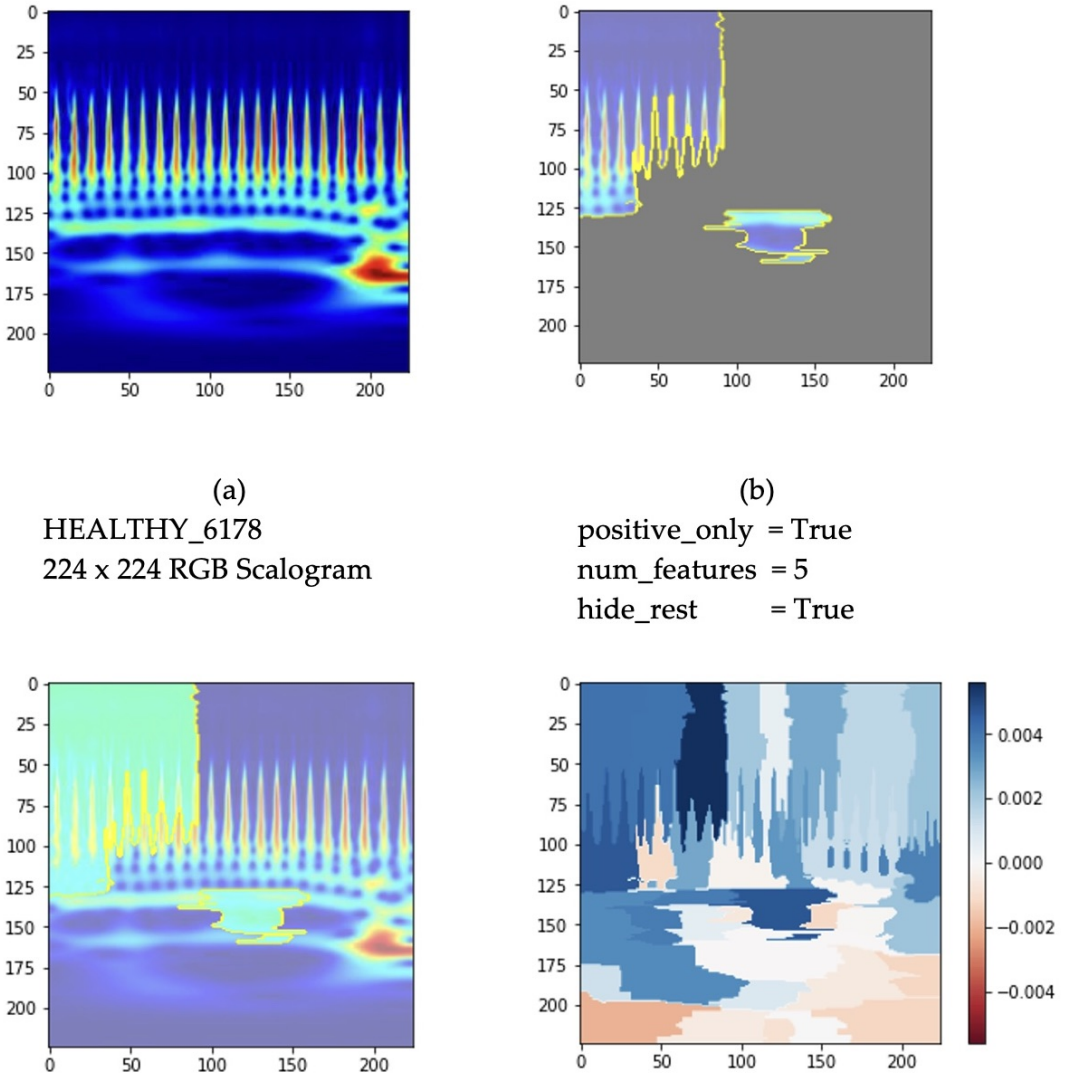

(a)
HEALTHY_6178
224 x 224 RGB Scalogram

(b)
positive_only = True
num_features = 5
hide_rest = True

(c)
positive_only = False
num_features = 5
hide_rest = False

(d)
Maping each explanation weight
to the corresponding superpixel

Figure 5.5 : LIME explanations: ECG of a healthy person, incorrectly classified as COPD with 99,4 % probability

5.9.2 SHapley Additive exPlanations (SHAP)

There are numerous techniques for enhancing model interpretability. SHAP Values is one of the most popular methods for describing the model and comprehending how the characteristics of data relate to its outputs. It is a method derived from game theory for distributing the "payout" evenly across the features. In other words, it utilizes game theory to assign credit for a model's prediction to each feature or feature value. SHAP Values provide both global and local explainability, which is one of their primary advantages.

In Figures 5.6, 5.7, 5.8, and 5.9, SHAP is used to explain the classification results of the fine-tuned VGG-19 model for randomly selected scalograms (COPD_3629, COPD_3650, COPD_3631, COPD_3640, COPD_3624, COPD_3607, COPD_3617, COPD_3591, HEALTHY_6570, HEALTHY_6577, HEALTHY_6564, HEALTHY_6401, HEALTHY_6223, HEALTHY_6185, HEALTHY_6191, HEALTHY_6198). In the first column are the scalograms to be explained. In the second column, explanations of the classes that the model determined are shown. The third column displays the other class's explanations. The red pixels represent the areas that cause the class determined by the model, while the blue pixels represent the exact opposite areas.

In Fig.5.9, intentionally selected the last four scalograms from those that contain extraordinary graphics. Here, it can be seen that the classification of the last three scalograms is incorrect. Considering the anomaly areas of these three scalograms, it can be stated that the model incorrectly classifies them due to the relatively abnormal areas.

When the SHAP explanations are examined, it is seen that the sections that positively affect the classification of healthy scalograms are located in the lower middle sections of the images. In HEALTHY_6185 and HEALTHY_6198, it can be seen that the misclassification is not caused by the anomalous parts that are prominent enough to be noticeable in the images, but the classification as COPD due to the effect of other parts in the scalograms.

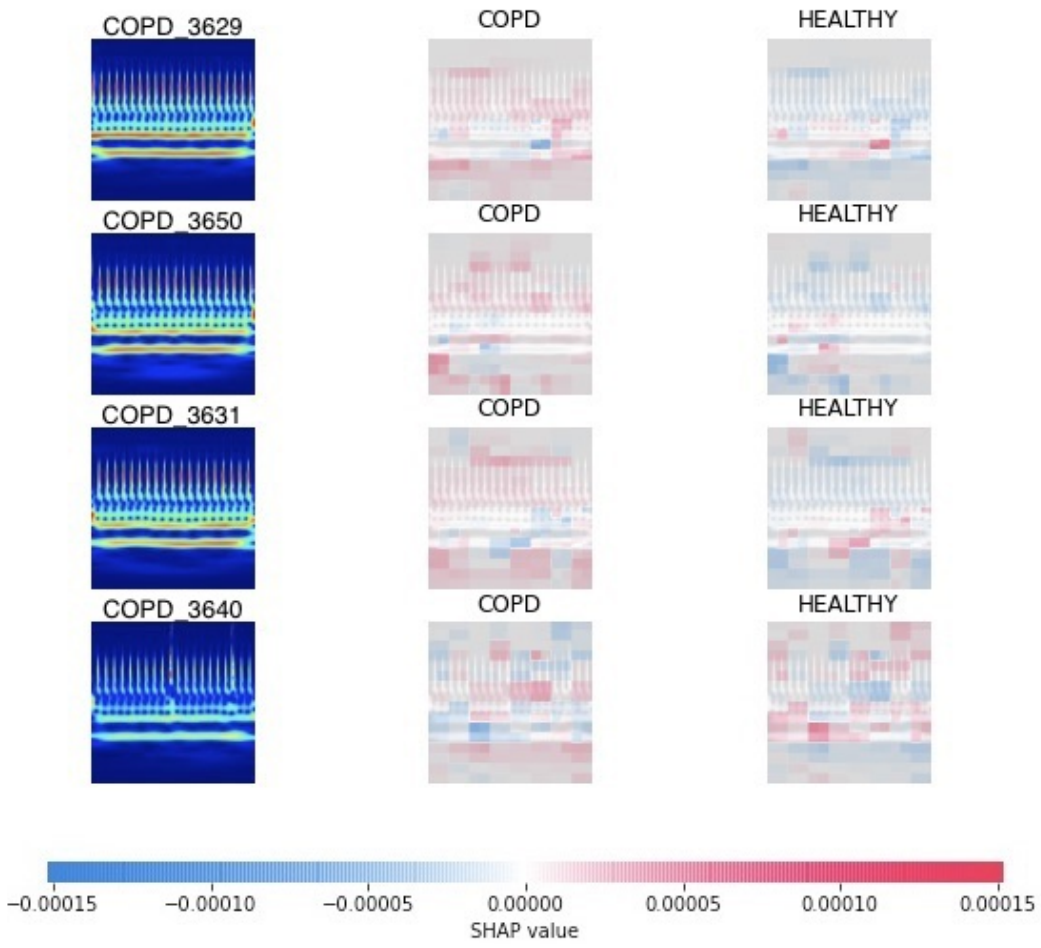

Figure 5.6 : Four scalograms with COPD and their SHAP explanations, all correctly classified

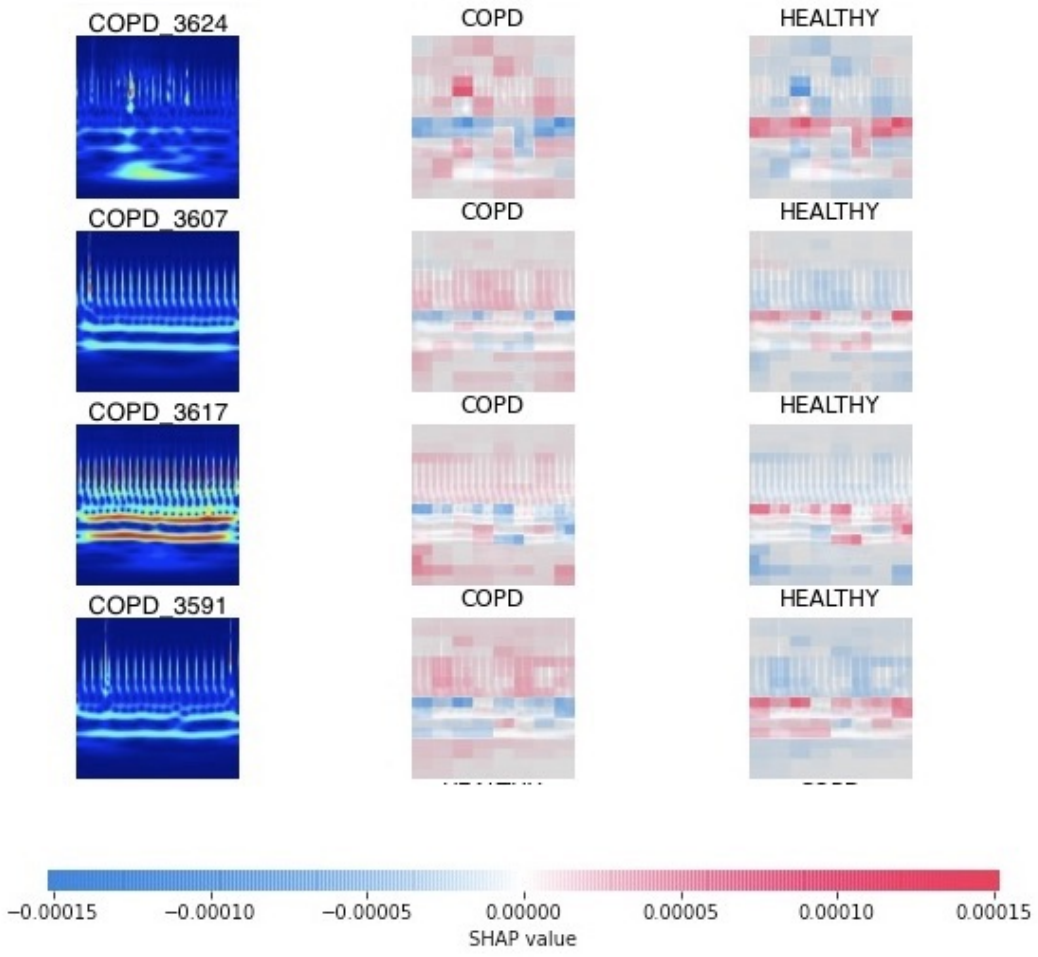

Figure 5.7 : Another four scalograms with COPD and their SHAP explanations, all correctly classified

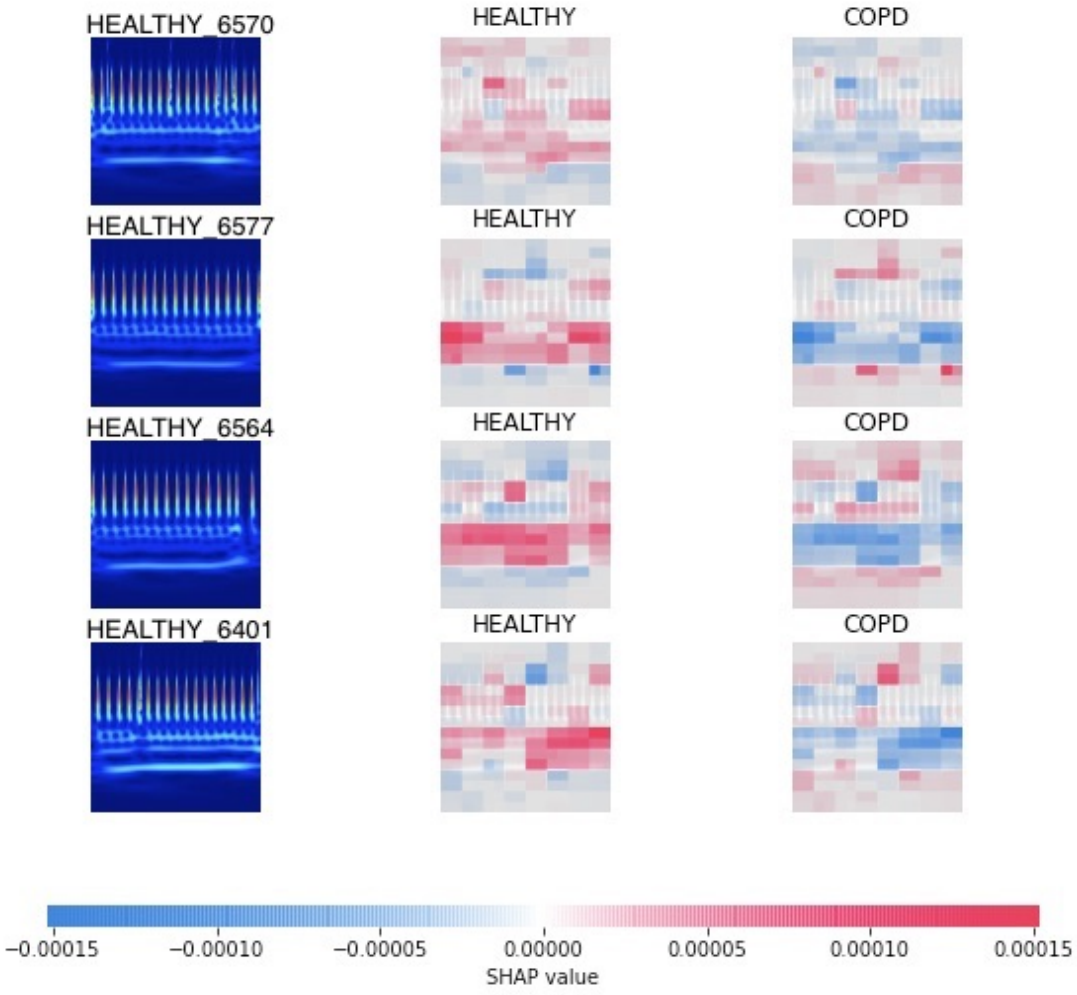

Figure 5.8 : Four scalograms of healthy group and their SHAP explanations, all correctly classified

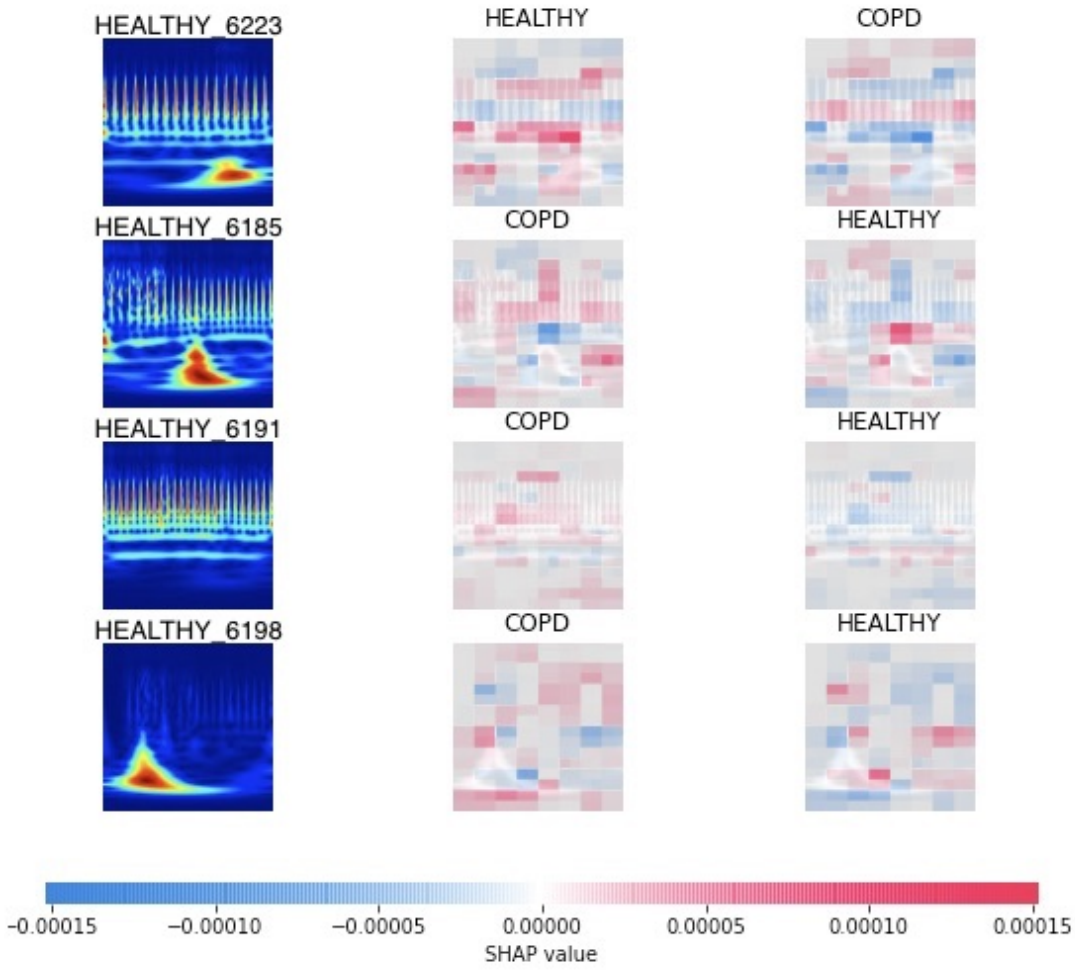

Figure 5.9 : Another four scalograms of healthy group and their SHAP explanations. The first one correctly classified, the last three incorrectly classified

6. CONCLUSIONS AND FUTURE WORK

As a result, this study has shed light on a number of important aspects of the research topic and has effectively addressed the research objectives outlined at the beginning of this thesis. We have achieved notable results and contributed significantly to the biomedical and computing fields through an in-depth evaluation of the suggested approach and a thorough investigation of the relevant literature. Our initial goal has been confirmed by the results. The findings have also revealed fresh directions for additional research and highlighted potential areas for it. The main conclusions of this study will be outlined in this chapter along with their implications and suggested future research avenues that can be used to further the understanding gained from this study.

6.1 Conclusions

Over the past few years, innovations such as machine learning and deep learning have been playing a pivotal role in delivering assistive remedies for healthcare challenges. In addition, they enhance the predictive accuracy of medical imaging for the early and timely detection of disease. The motivation of this thesis is that it introduces the first work on automated COPD diagnosis using deep learning and also utilizes the first annotated dataset in this field. As the disease progresses slowly and conceals itself until the final stage, hospital visits for diagnosis are uncommon. The medical goal of this thesis is to detect COPD using a simple heart signal before it becomes incurable. To address the COPD detection problem, we collected the ECG signals of 12 subjects, segmented them into 16 and 32-second long frames, transformed them to picture format using the signal transform methods, and then fed those images into CNNs. It is seen that Xception, fine-tuned VGG-19 and COPD Detector models give remarkable results while detecting COPD from ECG signals.

In addition to previous research in the literature, this thesis makes two contributions. The first is, low-cost, rapid, safe and automatic detection of the COPD disease achieved

using deep transfer learning. Since early prediction of COPD is vital to preventing the progression of the disease, the proposed method may give potential patients an opportunity to detect the disease at an early stage. Second, the findings suggest that future research should investigate the potential bio-marker behavior of the extracted features. The Xception model itself resulted in a performance that was nearly superior to other approaches that extracted features from non-medical images. This highlights the unique nature of the extracted features and identifies them as potential bio-markers.

6.2 Discussion

The utilization of the Jet colormap in coding phase is a commonly used practice in academic literature. This particular method is utilized during the conversion stage from a ECG signal to a scalogram. Each color is associated with a distinct level of intensity, and transitions occur between these colors. After careful analysis, it has been discovered that an alternative approach can be employed for the purpose of associating the transform coefficients with a colormap. As an alternative approach, it may also be efficient to carry out performance tests utilizing color maps such as 'parula' or viridis, which are also appropriate for visualizing quantitative data.

When considering color maps, it is important to note that the Jet color map consists of 256 distinct colors. In this particular context, each calculated CWT coefficient is assigned to the nearest color within the color map. The potential loss of detail can occur due to the mapping of similar CWT coefficients to the same color, depending on the data structure and color map employed. The visual representation of the CWT coefficients in the generated RGB image may not fully preserve the precise values of the coefficients.

One another potential source of decreased precision in the analysis is the process of quantization. Specifically, the CWT coefficients obtained for each segment of the signal undergo a conversion to uint8 format using the im2uint8 () function. The process of converting continuous values to discrete integer values within the range of 0 to 255 may result in a minor reduction in precision.

6.3 Future Work

At present, deep learning is being used throughout the entire medical image processing workflow, with impressive results in a variety of medical image analysis applications. In order to improve the early diagnosis and treatment of COPD, the use of deep learning technology to detect COPD using ECG signals to aid medical physicians is of considerable significance. The successful models can be put into practice and serve as a diagnostic aid for experts in chest diseases by providing objective and faster interpretation. It may be useful for medical decision-support tools to offer an extra option in difficult cases and can also be used to achieve a first assessment of the likelihood of illness in patients regardless of their symptoms.

This thesis contributes to the possibility of a low-cost, rapid, and automated COPD diagnosis that can be used clinically in the near future, as COPD is being diagnosed using an ECG signal instead of more time-consuming procedures such as transporting the patient to the hospital for a respiratory function test, CT scan, or MRI. This is also convenient and crucial for keeping patients away from infection hotspots, especially during pandemic or epidemic periods.

It must be noted that the results we observed were trustworthy and not the result of a specific architectural modification or technique. Therefore, four well-known and commonly used CNN model architectures are utilized with minimal modifications. With COPD Detector, five distinct CNN models are being investigated in total, and it is intended to research different deep network models, the selection of different hyper-parameters, loss functions, and optimizer functions to enhance the performance of COPD diagnosis. Future work may focus on developing more models structurally optimized for this task. Medical and computer scientists should also collaborate closely and employ their complementary expertise to confirm the utility of deep learning approaches.

The research also focuses on discovering possible Chronic Obstructive Pulmonary Disease related image biomarkers from scalograms derived from ECG signals. This thesis suggests that it might be possible to find new trustworthy bio-markers from ECG signal scalograms owing to the fact that outstanding classification results have

been obtained, even though the capacity of deep learning methods for image biomarker extraction is disputed due to the issue of interpretability. Due to the fact that the refined state-of-the-art CNNs depend on the evaluation of thousands of parameters to extract the key features, some of those factors could be actual image biomarkers, producing a trustworthy result. Future studies will examine this frontier, perhaps looking at other methods like radiomics [91].

In the data collection phase conducted in the sleep laboratory, the heart signal was acquired solely from a single channel. It is hypothesized that the discriminability of data collected from various channels may vary depending on the characteristics of the device employed in the context of COPD disease. It is suggested that future data collection studies should consider gathering data from multiple channels in order to enhance the comprehensiveness of the conducted investigations.

More patient data is needed for a more thorough analysis, especially for COPD patients. One of this thesis strengths is the use of AI to diagnose a fatal illness for which there is little human evidence. As previously noted, this research has some limitations that we want to resolve in the future. The subject pool is tiny, with 12 individuals. Although data augmentation could somewhat mitigate model overfitting and improve model performance, we will achieve better outcomes if we have access to additional data. To develop a larger dataset, we will continue to gather ECG data from COPD patients. Moreover, it is necessary to develop models capable of distinguishing COPD cases from other similar pulmonary or viral disease cases, such as pneumonia or emphysema.

Only two of the XAI methods, specifically LIME and SHAP, were taken into consideration in the research we conducted. Additional work is going to be done in the future with the goal of conducting in-depth analyses and establishing cause-and-effect relationships between diseases and the information contained in heart signals.

To further facilitate early illness diagnosis, it will be beneficial to include the COPD detection system into mobile and embedded devices as similar to the studies in the literature [92]. Future studies would be more fruitful if they focused on diagnosing COPD patients in their earliest stages, when they exhibit almost no symptoms.

It could also be put into practice and serve as a diagnostic aid for chest disease experts by providing a deeper and faster interpretation of ECG signals. Using the knowledge gained while identifying COPD from ECG signals may aid in the early diagnosis of future diseases for which little data is currently available.

In future research, the knowledge and expertise obtained from this thesis could also be used for other illness detection or classification problems besides COPD. The thesis is based on the premise that early diagnosis of COPD can reduce mortality rates throughout the world.

REFERENCES

[1] **Jones, P.W.**, **Vogelmeier, C.**, **Vestbo, J.**, **Hurd, S.S.**, **Agustı, A.G.**, **Anzueto, A.**, **Barnes, P.J.**, **Fabbri, L.M. and Martinez, F.J.** (2020). Pulmonary Perspective Global Strategy for the Diagnosis, Management, and Prevention of Chronic Obstructive Pulmonary Disease GOLD Executive Summary, *American journal of respiratory and critical care medicine*, *187 (4)*, 347–365.

[2] **Larssen, M.S.**, **Steine, K.**, **Hilde, J.M.**, **Skjørten, I.**, **Hodnesdal, C.**, **Liestøl, K. and Gjesdal, K.** (2017). Mechanisms of ECG signs in chronic obstructive pulmonary disease, *Heart*, *4*, 552, `http://openheart.bmj.com/`.

[3] **Moran, I.**, **Altilar, D.T.**, **Ucar, M.K.**, **Bilgin, C. and Bozkurt, M.R.** (2023). Deep Transfer Learning for Chronic Obstructive Pulmonary Disease Detection Utilizing Electrocardiogram Signals, *IEEE Access*, *11*, 40629–40644.

[4] **Peng, J.**, **Chen, C.**, **Zhou, M.**, **Xie, X.**, **Zhou, Y. and Luo, C.H.** (2020). A Machine-learning Approach to Forecast Aggravation Risk in Patients with Acute Exacerbation of Chronic Obstructive Pulmonary Disease with Clinical Indicators, *Scientific Reports*, *10 (1):3118*.

[5] **Westcott, A.**, **Capaldi, D.P.**, **McCormack, D.G.**, **Ward, A.D.**, **Fenster, A. and Parraga, G.** (2019). Chronic obstructive pulmonary disease: Thoracic CT texture analysis and machine learning to predict pulmonary ventilation, *Radiology*, *293*, 676–684.

[6] **Sun, J.**, **Liao, X.**, **Yan, Y.**, **Zhang, X.**, **Sun, J.**, **Tan, W.**, **Liu, B.**, **Wu, J.**, **Guo, Q.**, **Gao, S.**, **Li, Z.**, **Wang, K. and Li, Q.** (2022). Detection and staging of chronic obstructive pulmonary disease using a computed tomography-based weakly supervised deep learning approach, *Eur Radiology*, *32*, `https://doi.org/10.1007/s00330-022-08632-7`.

[7] **Sun, J.**, **Liao, X.**, **Yan, Y.**, **Zhang, X.**, **Sun, J.**, **Tan, W.**, **Liu, B.**, **Wu, J.**, **Guo, Q.**, **Gao, S.**, **Li, Z.**, **Wang, K. and Li, Q.** (2022). Detection and staging of chronic obstructive pulmonary disease using a computed tomography-based weakly supervised deep learning approach, *European Radiology*, *32*, 5319–5329, `https://doi.org/10.1007/s00330-022-08632-7`.

[8] **Siddiqui, H.U.R.**, **Raza, A.**, **Saleem, A.A.**, **Rustam, F.**, **Díez, I.d.l.T.**, **Aray, D.G.**, **Lipari, V.**, **Ashraf, I. and Dudley, S.** (2023). An Approach to Detect Chronic Obstructive Pulmonary Disease Using UWB Radar-Based Temporal and Spectral Features, *Diagnostics*, *13*(6), `https://www.mdpi.com/2075-4418/13/6/1096`.

[9] **Wu, C.T.**, **Li, G.H.**, **Huang, C.T.**, **Cheng, Y.C.**, **Chen, C.H.**, **Chien, J.Y.**, **Kuo, P.H.**, **Kuo, L.C. and Lai, F.** (2021). Acute Exacerbation of a Chronic Obstructive Pulmonary Disease Prediction System Using Wearable Device Data, Machine Learning, and Deep Learning: Development and Cohort Study, *JMIR Mhealth Uhealth*, *9*(5), e22591, `http://www.ncbi.nlm.nih.gov/pubmed/33955840`.

[10] **Altan, G.**, **Kutlu, Y. and Gökçen, A.** (2020). Chronic obstructive pulmonary disease severity analysis using deep learning on multi-channel lung sounds, *Turkish Journal of Electrical Engineering and Computer Sciences*, *28*, 2979–2996.

[11] **Zhang, B.**, **Wang, J.**, **Chen, J.**, **Ling, Z.**, **Ren, Y.**, **Xiong, D. and Guo, L.** (2023). Machine learning in chronic obstructive pulmonary disease, *Chinese Medical Journal*, *136*, 536–538.

[12] **Amaral, J.L.**, **Lopes, A.J.**, **Faria, A.C. and Melo, P.L.** (2015). Machine learning algorithms and forced oscillation measurements to categorise the airway obstruction severity in chronic obstructive pulmonary disease, *Computer Methods and Programs in Biomedicine*, *118*, 186–197.

[13] **Lyon, A.**, **Mincholé, A.**, **Martínez, J.P.**, **Laguna, P. and Rodriguez, B.** (2018). Computational techniques for ECG analysis and interpretation in light of their contribution to medical advances, *Journal of the Royal Society Interface*, *15(138):20170821*.

[14] **Llamedo, M. and Mart, J.P.** (2011). Heartbeat Classification Using Feature Selection driven by Database Generalization Criteria, *IEEE Transactions on Biomedical Engineering*, *58*, 616–625.

[15] **Chazal, P.D.**, **Reilly, R.B. and Member, S.** (2006). A Patient-Adapting Heartbeat Classifier Using ECG Morphology and Heartbeat Interval Features, *IEEE Transactions on Biomedical Engineering*, *53*, 2535–2543.

[16] **Übeyli, E.D.** (2007). ECG beats classification using multiclass support vector machines with error correcting output codes, *Digital Signal Processing*, *17*, 675–684.

[17] **Seera, M.**, **Lim, C.P.**, **Liew, W.S.**, **Lim, E. and Loo, C.K.** (2015). Classification of electrocardiogram and auscultatory blood pressure signals using machine learning models, *Expert Systems with Applications*, *42*, 3643–3652, `http://dx.doi.org/10.1016/j.eswa.2014.12.023`.

[18] **Kulesh, M.** (2011). Wavelet analysis, *Encyclopedia of Earth Sciences Series*, *Part 5*, 1517–1524.

[19] **Lecun, Y.**, **Bengio, Y. and Hinton, G.** (2015). Deep learning, *Nature*, *521*, 436–444.

[20] **Cheng, W.T. and Chan, K.L.** (1998). Classification of Electrocardiogram Using Hidden Markov Models, *Proceedings of the 20th Annual International Conference of the IEEE Engineering in Medicine and Biology Society*, *20*, 143–146.

[21] **Kachuee, M.**, **Fazeli, S. and Sarrafzadeh, M.** (2018). ECG heartbeat classification: A deep transferable representation, *Proceedings - 2018 IEEE International Conference on Healthcare Informatics, ICHI 2018*, pp.443–444.

[22] **Faust, O.**, **Hagiwara, Y.**, **Hong, T.J.**, **Lih, O.S. and Acharya, U.R.** (2018). Deep learning for healthcare applications based on physiological signals: A review, *Computer Methods and Programs in Biomedicine*, *161*, 1–13, https://doi.org/10.1016/j.cmpb.2018.04.005.

[23] **Hamza, M.A.**, **Mengash, H.A.**, **Alotaibi, S.S.**, **Hassine, S.B.H.**, **Yafoz, A.**, **Althukair, F.**, **Othman, M. and Marzouk, R.** (2022). Optimal and Efficient Deep Learning Model for Brain Tumor Magnetic Resonance Imaging Classification and Analysis, *Applied Sciences*, *12*, 7953.

[24] **Yaqub, M.**, **Jinchao, F.**, **Ahmed, S.**, **Arshid, K.**, **Bilal, M.A.**, **Akhter, M.P. and Zia, M.S.** (2022). GAN-TL: Generative Adversarial Networks with Transfer Learning for MRI Reconstruction, *Applied Sciences*, *12*, 8841, https://www.mdpi.com/2076-3417/12/17/8841.

[25] **M Ramadhan, A.B.** (2022). A Novel Approach to Detect COVID-19 : Enhanced Deep Learning Models with Convolutional Neural Networks, *Applied Sciences*, *12*.

[26] **Anwar, S.M.**, **Majid, M.**, **Qayyum, A.**, **Awais, M.**, **Alnowami, M. and Khan, M.K.** (2018). Medical Image Analysis using Convolutional Neural Networks: A Review, *Journal of Medical Systems*, *42*.

[27] **Wetteland, R.**, **Kvikstad, V.**, **Eftestol, T.**, **Tossebro, E.**, **Lillesand, M.**, **Janssen, E.A. and Engan, K.** (2021). Automatic diagnostic tool for predicting cancer grade in bladder cancer patients using deep learning, *IEEE Access*.

[28] **Kim, S.**, **Hahn, J.O. and Youn, B.D.** (2021). Deep Learning-Based Diagnosis of Peripheral Artery Disease via Continuous Property-Adversarial Regularization: Preliminary in Silico Study, *IEEE Access*, *9*, 127433–127443.

[29] **Alghamdi, H.S.**, **Amoudi, G.**, **Elhag, S.**, **Saeedi, K. and Nasser, J.** (2021). Deep Learning Approaches for Detecting COVID-19 from Chest X-Ray Images: A Survey, *IEEE Access*, *9*, 20235–20254.

[30] **Zhou, C.**, **Song, J.**, **Zhou, S.**, **Zhang, Z. and Xing, J.** (2021). COVID-19 Detection based on Image Regrouping and ResNet-SVM using Chest X-ray Images, *IEEE Access*.

[31] **da S. Luz, E.J.**, **Schwartz, W.R.**, **Cámara-Chávez, G. and Menotti, D.** (2016). ECG-based heartbeat classification for arrhythmia detection: A survey, *Computer Methods and Programs in Biomedicine*, *127*, 144–164, `http://dx.doi.org/10.1016/j.cmpb.2015.12.008`.

[32] **Yildirim, O.**, **Baloglu, U.B.**, **Tan, R.S.**, **Ciaccio, E.J. and Acharya, U.R.** (2019). A new approach for arrhythmia classification using deep coded features and LSTM networks, *Computer Methods and Programs in Biomedicine*, *176*, 121–133.

[33] **Porumb, M.**, **Iadanza, E.**, **Massaro, S. and Pecchia, L.** (2020). A convolutional neural network approach to detect congestive heart failure, *Biomedical Signal Processing and Control*.

[34] **Shi, H.**, **Wang, H.**, **Qin, C.**, **Zhao, L. and Liu, C.** (2020). An incremental learning system for atrial fibrillation detection based on transfer learning and active learning, *Computer Methods and Programs in Biomedicine*, *187*, 105219, `https://doi.org/10.1016/j.cmpb.2019.105219`.

[35] **Uçar, M.K.**, **Moran, İ.**, **Altılar, D.T.**, **Bilgin, C. and Bozkurt, M.R.** (2018). Statistical Analysis of The Relationship Between Chronic Obstructive Pulmonary Disease and Electrocardiogram Signal, *Journal of Human Rhythm*, *4*(3), 142 – 149.

[36] **Moran, İ.**, **Uçar, M.K.**, **Altılar, D.T.**, **Bilgin, C. and Bozkurt, M.R.** (2018). Rule-based diagnosis of chronic obstructive pulmonary disease with electrocardiogram signal, *2018 Electric Electronics, Computer Science, Biomedical Engineerings' Meeting (EBBT)*, pp.1–5.

[37] **Qureshi, H.**, **Sharafkhaneh, A. and Hanania, N.A.** (2014). Chronic obstructive pulmonary disease exacerbations: Latest evidence and clinical implications, *Therapeutic Advances in Chronic Disease*, *5*, 212–227.

[38] **Ichikawa, A.**, **Matsumura, Y.**, **Ohnishi, H.**, **Kataoka, H.**, **Ogura, K.**, **Yokoyama, A. and Sugiura, T.** (2016). Identification of electrocardiographic values that indicate chronic obstructive pulmonary disease, *Heart and Lung: Journal of Acute and Critical Care*, *45*, 359–362, `http://dx.doi.org/10.1016/j.hrtlng.2016.04.004`.

[39] **Bajaj, R.**, **Chhabra, L.**, **Basheer, Z. and Spodick, D.H.** (2013). Optimal electrocardiographic limb lead set for rapid emphysema screening, *International Journal of COPD*, *8*, 41–44.

[40] **Mincholé, A.**, **Camps, J.**, **Lyon, A. and Rodríguez, B.** (2019). Machine learning in the electrocardiogram, *Journal of Electrocardiology*, *57*.

[41] **Madias, J.E.** (2008). Low QRS voltage and its causes, *Journal of Electrocardiology*, *41*, 498–500.

[42] **Chhabra, L.**, **Sareen, P.**, **Perli, D.**, **Srinivasan, I. and Spodick, D.H.** (2012). Vertical P-wave axis: The electrocardiographic synonym for pulmonary emphysema and its severity, *Indian Heart Journal*, *64*, 40–42, http://dx.doi.org/10.1016/S0019-4832(12)60009-1.

[43] **Fowler, N.O.**, **Daniels, C.**, **Scott, R.C.**, **Faustino, B.S. and Gueron, M.** (1965). The electrocardiogram in cor pulmonale with and without emphysema, *The American Journal of Cardiology*.

[44] **Padmavati, S. and Raizada, V.** (1972). Electrocardiogram in chronic cor pulmonale, *Heart*, *34*, 658–667.

[45] **Yildirim, O.**, **Talo, M.**, **Ay, B.**, **Baloglu, U.B.**, **Aydin, G. and Acharya, U.R.** (2019). Automated detection of diabetic subject using pre-trained 2D-CNN models with frequency spectrum images extracted from heart rate signals, *Computers in Biology and Medicine*, *113*, 103387, https://doi.org/10.1016/j.compbiomed.2019.103387.

[46] **Nasrabadi, N.M.** (2007). Pattern Recognition and Machine Learning, *Journal of Electronic Imaging*, *16*(4), 049901, https://doi.org/10.1117/1.2819119.

[47] **Samuel, A.L.** (1959). Some Studies in Machine Learning Using the Game of Checkers, *IBM Journal of Research and Development*, *3*(3), 210–229.

[48] **Bishop, C.M.** (2007). *Pattern Recognition and Machine Learning (Information Science and Statistics)*, Springer, 1 edition.

[49] **Chapelle, O.**, **Schölkopf, B. and Zien, A.** (2006). *Semi-Supervised Learning*, The MIT Press, http://dblp.uni-trier.de/db/books/collections/CSZ2006.html.

[50] **Bengio, Y.** (2012). Practical recommendations for gradient-based training of deep architectures, *Arxiv*.

[51] **Krizhevsky, A.**, **Sutskever, I. and Hinton, G.E.** (2012). ImageNet Classification with Deep Convolutional Neural Networks, *Advances in Neural Information Processing Systems*, 25, 1106 – 1114, https://papers.nips.cc/paper/4824-imagenet-classification-with-deep-convolutional-neural-pdf.

[52] **Lecun, Y.**, **Bottou, L.**, **Bengio, Y. and Haffner, P.** (1998). Gradient-Based Learning Applied to Document Recognition, *Proceedings of the IEEE*, *86*, 2278 – 2324.

[53] **Zeiler, M.D. and Fergus, R.** (2014). Visualizing and Understanding Convolutional Networks, ***D. Fleet, T. Pajdla, B. Schiele and T. Tuytelaars**, editors, Computer Vision – ECCV 2014*, Springer International Publishing, Cham, pp.818–833.

[54] **Simonyan, K. and Zisserman, A.** (2014). Very Deep Convolutional Networks for Large-Scale Image Recognition, *arXiv 1409.1556*.

[55] **Szegedy, C.**, **Liu, W.**, **Jia, Y.**, **Sermanet, P.**, **Reed, S.**, **Anguelov, D.**, **Erhan, D.**, **Vanhoucke, V. and Rabinovich, A.** (2014). *Going Deeper with Convolutions*, `1409.4842`.

[56] **Lin, M.**, **Chen, Q. and Yan, S.** (2014). Network In Network, *Network In Network*, p. 10.

[57] **Songtao, W.**, **Zhong, S. and Liu, Y.** (2018). Deep residual learning for image steganalysis, *Multimedia Tools and Applications*, *77*.

[58] **Girshick, R.**, **Donahue, J.**, **Darrell, T. and Malik, J.** (2013). Rich Feature Hierarchies for Accurate Object Detection and Semantic Segmentation, *Proceedings of the IEEE Computer Society Conference on Computer Vision and Pattern Recognition*, 580–587.

[59] **He, K.**, **Gkioxari, G.**, **Dollár, P. and Girshick, R.** (2017). Mask R-CNN, *2017 IEEE International Conference on Computer Vision (ICCV)*, pp.2980–2988.

[60] **Heaton, J.** (2017). Ian Goodfellow, Yoshua Bengio, and Aaron Courville Deep learning: The MIT Press, 2016, 800 pp, ISBN: 0262035618, *Genetic Programming and Evolvable Machines*, *19*.

[61] **Bengio, Y.** (2009). Learning Deep Architectures for AI, *Foundations and trends in Machine Learning*, *2*, 1–55.

[62] **McCulloch, W.S. and Pitts, W.** (1943). A logical calculus of the ideas immanent in nervous activity, *Bulletin of mathematical biophysics*, *5*(4), 115–133.

[63] **Krenker, A.**, **Bester, J. and Kos, A.** (2011). Introduction to the Artificial Neural Networks, pp.3–18.

[64] **Celik, Y.**, **Talo, M.**, **Yildirim, O.**, **Karabatak, M. and Acharya, U.R.** (2020). Automated invasive ductal carcinoma detection based using deep transfer learning with whole-slide images, *Pattern Recognition Letters*, *133*, 232–239, `https://doi.org/10.1016/j.patrec.2020.03.011`.

[65] **Celli, B.R.**, **MacNee, W.**, **Agusti, A.**, **Anzueto, A.**, **Berg, B.**, **Buist, A.S.**, **Calverley, P.M.**, **Chavannes, N.**, **Dillard, T.**, **Fahy, B.**, **Fein, A.**, **Heffner, J.**, **Lareau, S.**, **Meek, P.**, **Martinez, F.**, **McNicholas, W.**, **Muris, J.**, **Austegard, E.**, **Pauwels, R.**, **Rennard, S.**, **Rossi, A.**, **Siafakas, N.**, **Tiep, B.**, **Vestbo, J.**, **Wouters, E. and ZuWallack, R.** (2004). Standards for the diagnosis and treatment of patients with COPD: A summary of the ATS/ERS position paper, *European Respiratory Journal*, *23*, 932–946.

[66] **Zhuang, F.**, **Qi, Z.**, **Duan, K.**, **Xi, D.**, **Zhu, Y.**, **Zhu, H.**, **Xiong, H. and He, Q.** (2020). A Comprehensive Survey on Transfer Learning, *Proceedings of the IEEE*, *PP*, 1–34.

[67] **Pan, S.J. and Yang, Q.** (2010). A Survey on Transfer Learning, *IEEE Transactions on Knowledge and Data Engineering*, *22*(10), 1345–1359.

[68] **Weiss, K.**, **Khoshgoftaar, T.M. and Wang, D.D.** (2016). A survey of transfer learning, *Journal of Big Data*, *3*.

[69] **Thrun, S. and Pratt, L.** (1998). Learning to Learn: Introduction and Overview, Springer US, Boston, MA, pp.3–17, `https://doi.org/10.1007/978-1-4615-5529-2_1`.

[70] **Caruana, R.** (1997). Multitask Learning, *Machine Learning*, *28*, 41–75.

[71] **Duan, L.**, **Xu, D. and Tsang, I.W.H.** (2012). Learning with Augmented Features for Heterogeneous Domain Adaptation, *ArXiv*, *abs/1206.4660*.

[72] **Kulis, B.**, **Saenko, K. and Darrell, T.** (2011). *What you saw is not what you get: Domain adaptation using asymmetric kernel transforms*, pp.1785 – 1792.

[73] **Zhu, Y.**, **Chen, Y.**, **Lu, Z.**, **Pan, S.**, **Xue, G.R.**, **Yu, Y. and Yang, Q.** (2011). Heterogeneous Transfer Learning for Image Classification, volume 2.

[74] **Nam, J.**, **Fu, W.**, **Kim, S.**, **Menzies, T. and Tan, L.** (2017). Heterogeneous Defect Prediction, *IEEE Transactions on Software Engineering*, *PP*, 1–1.

[75] **Wang, C. and Mahadevan, S.** (2011). Heterogeneous Domain Adaptation Using Manifold Alignment, *International Joint Conference on Artificial Intelligence*.

[76] **Harel, M. and Mannor, S.** (2010). Learning from Multiple Outlooks, *Computing Research Repository - CORR*.

[77] **Zhou, J.T.**, **W.Tsang, I.**, **Pan, S.J. and Tan, M.** (2014). Heterogeneous Domain Adaptation for Multiple Classes, ***S. Kaski and J. Corander**, editors, Proceedings of the Seventeenth International Conference on Artificial Intelligence and Statistics*, volume 33 of *Proceedings of Machine Learning Research*, PMLR, Reykjavik, Iceland, pp.1095–1103, `https://proceedings.mlr.press/v33/zhou14.html`.

[78] **Prettenhofer, P. and Stein, B.** (2010). Cross-Language Text Classification Using Structural Correspondence Learning, *Proceedings of the 48th Annual Meeting of the Association for Computational Linguistics*, ACL '10, Association for Computational Linguistics, USA, p.1118–1127.

[79] **Zhou, J.**, **Pan, S.**, **Tsang, I. and Yan, Y.** (2014). Hybrid Heterogeneous Transfer Learning through Deep Learning, *Proceedings of the AAAI Conference on Artificial Intelligence*, *28*.

[80] **Wei, D. and Zhang, Y.** (2021). Fractional Stockwell transform: Theory and applications, *Digital Signal Processing*, *115*, 103090, https://www.sciencedirect.com/science/article/pii/S1051200421001299.

[81] **Shyu, L.Y.**, **Wu, Y.H. and Hu, W.** (2004). Using wavelet transform and fuzzy neural network for VPC detection from the holter ECG, *IEEE Transactions on Biomedical Engineering*, *51*, 1269–1273.

[82] **Bellanger, J.J. and G. Passariello L. Senhadji, G.C.** (1995). Comparing Wavelet Transforms for Recognizing Cardiac Patterns, *IEEE Engineering in Medicine and Biology Magazine*, *14*, 167–173.

[83] **Wang, G.**, **Li, W.**, **Zuluaga, M.A.**, **Pratt, R.**, **Patel, P.A.**, **Aertsen, M.**, **Doel, T.**, **David, A.L.**, **Deprest, J.**, **Ourselin, S. and Vercauteren, T.** (2018). Interactive Medical Image Segmentation Using Deep Learning with Image-Specific Fine Tuning, *IEEE Transactions on Medical Imaging*, *37*, 1562–1573.

[84] **Stockwell, R.**, **Mansinha, L. and Lowe, R.** (1996). Localization of the complex spectrum: The S transform, *IEEE Transactions on Signal Processing*, *44*(4), 998 – 1001, https://www.scopus.com/inward/record.uri?eid=2-s2.0-0030127735&doi=10.11092f78.492555&partnerID=40&md5=3e59d5100ab7715eb0bd4660f5b51acc, cited by: 2542.

[85] **Raj, S.and Phani, T. and Dalei, J.** (2016). Power quality analysis using modified S -transform on ARM processor, *2016 Sixth International Symposium on Embedded Computing and System Design (ISED)*, pp.116–170.

[86] **Zhao, Z.**, **Wang, S.**, **Zhang, W. and Xie, Y.** (2016). A novel automatic modulation classification method based on Stockwell -transform and energy entropy for underwater acoustic signals, *IEEE international conference on signal processing, communications and computing (ICSPCC)*, pp.1–6.

[87] **Yang, Y.**, **Yan, L.F.**, **Zhang, X.**, **Han, Y.**, **Nan, H.Y.**, **Hu, Y.C.**, **Hu, B.**, **Yan, S.L.**, **Zhang, J.**, **Cheng, D.L.**, **Ge, X.W.**, **Cui, G.B.**, **Zhao, D. and Wang, W.** (2018). Glioma grading on conventional MR images: A deep learning study with transfer learning, *Frontiers in Neuroscience*, *12*, 1–10.

[88] **Shin, H.C.**, **Roth, H.R.**, **Gao, M.**, **Lu, L.**, **Xu, Z.**, **Nogues, I.**, **Yao, J.**, **Mollura,** D. **and Summers, R.M.** (2016). Deep Convolutional Neural Networks for Computer-Aided Detection: CNN Architectures, Dataset Characteristics and Transfer Learning, *IEEE Transactions on Medical Imaging*, *35*, 1285–1298.

[89] **Ribeiro, M.T.**, **Singh, S. and Guestrin, C.** (2016). "Why Should I Trust You?": Explaining the Predictions of Any Classifier, *Proceedings of the 22nd ACM SIGKDD International Conference on Knowledge Discovery and Data Mining*, KDD '16, Association for Computing Machinery, New York, NY, USA, p.1135–1144, https://doi.org/10.1145/2939672.2939778.

[90] **Lundberg, S.M. and Lee, S.I.** (2017). A Unified Approach to Interpreting Model Predictions, *Proceedings of the 31st International Conference on Neural Information Processing Systems*, NIPS'17, Curran Associates Inc., Red Hook, NY, USA, p.4768–4777.

[91] **Parekh, V.S. and Jacobs, M.A.** (2019). Deep learning and radiomics in precision medicine, *Precision Medicine and Drug Development*, *4*, 59–72.

[92] **Srivastava, A.**, **Jain, S.**, **Miranda, R.**, **Patil, S.**, **Pandya, S. and Kotecha, K.** (2021). Deep learning based respiratory sound analysis for detection of chronic obstructive pulmonary disease, *PeerJ Computer Science*, *7*, 1–22.

CURRICULUM VITAE

İnanç MORAN

EDUCATION:

- **B.Sc.:** 2000, Turkish Naval Academy, Computer Engineering Department
- **M.Sc.:** 2005, Naval Sciences and Engineering Institute, Computer Engineering Department
- **M.Sc.:** 2007, Beykent University, Department of Business Administration

PROFESSIONAL EXPERIENCE:

- 2019-Present, IT Manager, Turkish National Defense University, Istanbul, Turkey
- 2016-2019, ICT Manager, Naval Training Center Command, Yalova, Turkey
- 2018, IT Advisor to Afghanistan Ministry of Defence, NATO Resolute Support Headquarters, Kabul, Afghanistan
- 2010-2016, System Manager, Naval Training and Education Command, Istanbul, Turkey
- 2008-2010, IT Manager, Office of Navigation, Hydrography and Oceanography, Istanbul, Turkey
- 2009, Visiting Researcher, NATO Centre for Maritime Research and Experimentation, La Spezia, Italy
- 2005-2008, System And Network Administrator, Turkish Northern Sea Area Command, Istanbul, Turkey
- 2003-2005, Researcher, Naval Sciences and Engineering Institute, Istanbul, Turkey
- 2000-2003, Navy Officer, Turkish Naval Forces, Turkey

PUBLICATIONS, PRESENTATIONS AND PATENTS ON THE THESIS:

- **Moran I.**, Altilar D.T., Ucar M.K., Bilgin, C., Bozkurt M.R., (2023). Deep Transfer Learning for Chronic Obstructive Pulmonary Disease Detection Utilizing Electrocardiogram Signals. *IEEE Access,* vol. 11, pp. 40629-40644, 2023, doi: 10.1109/ACCESS.2023.3269397.

- Ucar M.K., **Moran I.**, Altilar D.T., Bilgin, C., Bozkurt M.R., (2018). Rule-based Diagnosis of Chronic Obstructive Pulmonary Disease with Electrocardiogram Signal. *2018 Electric Electronics, Computer Science, Biomedical Engineerings Meeting (EBBT)*, April 18-19, 2018 Istanbul, Turkey. pp. 1-5, doi: 10.1109/EBBT.2018.8391462.
- Ucar M.K., **Moran I.**, Altilar D.T., Bilgin, C., Bozkurt M.R., (2018). Statistical Analysis of The Relationship Between Chronic Obstructive Pulmonary Disease and Electrocardiogram Signal. *Journal of Human Rhythm,* vol. 4, no. 3, pp. 142-149, 2018, doi: 10.1109/EBBT.2018.8391462.

OTHER PUBLICATIONS, PRESENTATIONS AND PATENTS:

- **Moran I.**, Altilar D.T., (2005). Three Plane Approach for 3D True Proportional Navigation. *AIAA Guidance, Navigation, and Control Conference and Exhibit,* August 15-18, 2005 San Francisco, USA, p. 6457, doi: 10.2514/6.2005-6457.